Redox Biology 72 (2024) 103127

Contents lists available at ScienceDirect

Redox Biology

journal homepage: www.elsevier.com/locate/redox

The redox-sensitive GSK3β is a key regulator of glomerular podocyte injury in type 2 diabetic kidney disease

Mengxuan Chen [a], Yudong Fang [a], Yan Ge [a], Shuhao Qiu [a], Lance Dworkin [a,b], Rujun Gong [a,b,c,*]

[a] Division of Nephrology, Department of Medicine, University of Toledo College of Medicine, Toledo, OH, USA
[b] Department of Physiology and Pharmacology, University of Toledo College of Medicine, Toledo, OH, USA
[c] Center for Diabetes and Endocrine Research, University of Toledo Medical Center, Toledo, OH, USA

ARTICLE INFO

Keywords:
Diabetic kidney disease
Diabetic podocytopathy
Insulin pathway
Antioxidant response
Cellular senescence

ABSTRACT

Emerging evidence suggests that GSK3β, a redox-sensitive transducer downstream of insulin signaling, acts as a convergent point for myriad pathways implicated in kidney injury, repair, and regeneration. However, its role in diabetic kidney disease remains controversial. In cultured glomerular podocytes, exposure to a milieu of type 2 diabetes elicited prominent signs of podocyte injury and degeneration, marked by loss of homeostatic marker proteins like synaptopodin, actin cytoskeleton disruption, oxidative stress, apoptosis, and stress-induced premature senescence, as shown by increased staining for senescence-associated β-galactosidase activity, amplified formation of γH2AX foci, and elevated expression of mediators of senescence signaling, like p21 and $p16^{INK4A}$. These degenerative changes coincided with GSK3β hyperactivity, as evidenced by GSK3β overexpression and reduced inhibitory phosphorylation of GSK3β, and were averted by tideglusib, a highly-selective small molecule inhibitor of GSK3β. In agreement, *post-hoc* analysis of a publicly-available glomerular transcriptomics dataset from patients with type 2 diabetic nephropathy revealed that the curated diabetic nephropathy-related gene set was enriched in high GSK3β expression group. Mechanistically, GSK3β-modulated nuclear factor Nrf2 signaling is involved in diabetic podocytopathy, because GSK3β knockdown reinforced Nrf2 antioxidant response and suppressed oxidative stress, resulting in an improvement in podocyte injury and senescence. Conversely, ectopic expression of the constitutively active mutant of GSK3β impaired Nrf2 antioxidant response and augmented oxidative stress, culminating in an exacerbated diabetic podocyte injury and senescence. Moreover, IRS-1 was found to be a cognate substrate of GSK3β for phosphorylation at $IRS\text{-}1^{S332}$, which negatively regulates IRS-1 activity. GSK3β hyperactivity promoted IRS-1 phosphorylation, denoting a desensitized insulin signaling. Consistently, *in vivo* in *db/db* mice with diabetic nephropathy, GSK3β was hyperactive in glomerular podocytes, associated with IRS-1 hyperphosphorylation, impaired Nrf2 response and premature senescence. Our finding suggests that GSK3β is likely a novel therapeutic target for treating type 2 diabetic glomerular injury.

As one of the most common complications of diabetes, diabetic kidney disease (DKD) has been the leading cause of end stage renal failure in the U.S. and other Western societies for several decades [1], and its prevalence is steadily increasing in developing countries [2]. Currently, the standard clinical treatment of DKD is largely confined to the use of renin–angiotensin–aldosterone system blockades, which may help slow but cannot halt the progression of DKD [3,4]. Recent development and clinical trials of a number of novel therapeutics, such as sodium/glucose cotransporter-2 inhibitors [5,6], glucagon-like peptide-1 receptor agonists [7] and nonsteroidal mineralocorticoid receptor antagonists [8], have shown promising results and may provide additional treatment options for DKD. However, their true efficacy and safety in DKD patients require in-depth testing through large-scale clinical trials. Clinical managements of DKD remain a challenge, especially for patients at high risk of progression [9]. It is imperative to improve our understanding of the pathogenic mechanisms of DKD and identify novel therapeutic targets.

The hallmark of diabetic nephropathy (DN) is persistent excessive urinary albumin excretion followed by insidious loss of kidney function that may start many years before the development of symptoms [10]. As a matter of fact, clinical staging of DN has been largely based on the severity of albuminuria, ranging from normoalbuminuria and

* Corresponding author. Division of Nephrology, University of Toledo Medical Center, 3000 Arlington Ave, Toledo, 43614, Ohio, USA.
E-mail address: Rujun.Gong@UToledo.edu (R. Gong).

https://doi.org/10.1016/j.redox.2024.103127
Received 7 February 2024; Received in revised form 6 March 2024; Accepted 15 March 2024
Available online 16 March 2024

microalbuminuria in the incipient or early stage to macroalbuminuria and later overt proteinuria in the advanced stage [11]. Urinary excretion of albumin is meticulously controlled by glomerular permselectivity that is achieved *via* a special histological structure in renal glomeruli termed glomerular filtration barrier, which is composed of fenestrated glomerular endothelia, glomerular basement membrane and glomerular podocytes. As the core structural component of the glomerular filtration barrier, glomerular podocytes are highly arborized and terminally differentiated cells with elaborate interdigitating foot processes that envelop the glomerular capillary tufts and impede protein in the bloodstream from leaking into the urine [12]. Converging evidence suggests that podocyte injury is a major culprit for proteinuria and progressive glomerular destruction in all proteinuric glomerular diseases including DN [13,14]. While the key pathogenic mechanisms driving the progression of DN remain unclear, podocyte injury and loss has been shown as a strong predictor of progressive DN, and the degree of podocyte injury and reduction correlates directly with the magnitude of proteinuria [15]. Therefore, therapeutic strategies targeting podocyte injury and loss would be a mechanism-based approach to prevent albuminuria and to slow the progression of DN.

Burgeoning evidence suggests that glycogen synthase kinase (GSK) 3β plays a critical role in podocyte disease and health [16–18]. GSK3 is a highly conserved, redox-sensitive serine/threonine protein kinase [19] that was originally characterized to be a key transducer of the insulin signaling pathway and regulate glycogen biogenesis [20]. As a multitasking kinase, GSK3 also acts as a convergent point for multiple pathways involved in organ injury, repair, and regeneration, and plays a pivotal role in a number of signaling cascades, including the β-catenin pathway, the nuclear factor-κB (NF-κB) pathway, nuclear factor erythroid 2–related factor 2 (Nrf2) antioxidant response, and cellular senescence pathways [21,22]. GSK3 exists in 2 isoforms (α and β) that are differentially expressed in different tissues [23]. The β rather than the α isoform of GSK3 is predominantly expressed in glomeruli and highly enriched in podocytes [24]. Evidence suggests that podocyte GSK3 is an evolutionarily conserved critical regulator of kidney function. To this end, combined knockout (KO) of both GSK3α and GSK3β specifically in glomerular podocytes in embryonic or adult mice caused severe podocyte injury, glomerulosclerosis, and heavy proteinuria [25]. However, in stark contrast, podocyte-specific KO of only GSK3β in mice either at the embryonic stage or during young adulthood resulted in no discernible phenotype [16,25]. Instead, KO of GSK3β in podocytes protected against glomerular injury and proteinuria in nondiabetic glomerular diseases [26], including Adriamycin nephropathy and nephrotoxic serum nephritis [17,27]. In patients with DKD, GSK3β is overexpressed and hyperactive in podocytes, correlating with the severity and progression of DKD [28]. However, it remains elusive whether GSK3β is involved in podocyte injury in diabetes, in particular type 2 diabetes mellitus, which accounts for approximately 90% to 95% of all diagnosed cases of diabetes. This study aimed to address this issue by utilizing an *in vitro* model of diabetic podocyte injury in cultured podocytes exposed to a milieu of type 2 diabetes. Key findings were further validated *in vivo* in *db/db* mice with DN. In addition, the effect of pharmacological targeting of GSK3β was tested by using tideglusib (TDG), the first clinically relevant highly selective small molecule inhibitor of GSK3β that has completed Phase II clinical trial and proven safe and well tolerated [29,30].

1. Materials and methods

1.1. Cell culture and treatment

Conditionally immortalized mouse podocytes were cultured in RPMI 1640 medium containing 10% FBS in a humidified incubator with 5% CO_2 as described previously [31]. After 14 days of differentiation, differentiated podocytes were exposed either to normal culture medium containing 5 mM glucose and 20 mM mannitol as an osmotic control or to a type 2 diabetic milieu consisting of 25 mM D-glucose (Sigma-Aldrich, St. Louis, MO, USA), 1 ng/ml tumor necrosis factor α (TNF-α, Abcam, Waltham, MA, USA), 1 ng/ml interleukin 6 (IL-6, Abcam) and 100 nM insulin (Thermo Fisher, Waltham, MA, USA) in the presence or absence of TDG (Shelleckchem, Houston, TX, USA) for 48 h. The dose of TDG was selected based on previous studies [32,33] after optimization by pilot experiments.

1.2. Transient transfection and RNA interference (RNAi)

To obtain podocytes expressing high levels of GSK3β, the plasmid vector encoding the hemagglutinin (HA)-tagged constitutively active mutant (S9A) of GSK3β was transfected into podocytes using the Lipofectamine 3000 reagent (Thermo Fisher), and podocytes transfected with the empty plasmid vector (EV) served as controls as described previously [34–36]. To knock down GSK3β, a sequence-specific RNAi directly against GSK3β (siGSK3β, Santa Cruz Biotechnology, Inc, Dallas, TX, USA) was transfected to podocytes, and tested against control RNAi using a scrambled RNAi construct (siCtrl, Santa Cruz Biotechnology, Inc.). After transfection, cells were treated with type 2 diabetic milieu in the presence or absence of tert-butylhydroquinone (tBHQ, 20 μM, Sigma-Aldrich) or trigonelline (Trig, 30 μM, Sigma-Aldrich) for 48 h as previously described [22].

1.3. Animal experimental design

All animal experiments and procedures were approved by the University of Toledo Institutional Animal Care and Use Committee and conformed to the regulations of the US Department of Agriculture and the National Institutes of Health *Guide for the Care and Use of Laboratory Animals*. BKS.Cg-*Dock7*$^{m\ +/+}$ *Lepr*^{db}/J (*db/m*) mice were purchased from the Jackson Laboratory (#000642, Bar Harbor, ME, USA) and bred to homozygosity to obtain BKS.Cg-*Dock7*^{m} *Lepr*$^{db/+\ +}$/J (*db/db*) mice as described previously [37]. Mice were given food and water *ad libitum*. They were euthanized at 16 weeks, and urine samples and kidneys were collected.

1.4. Genotyping of mice

Ear punch tissues from mice were used for the extraction of genomic DNA as previously described [38]. Genotyping was performed by using tetra-primer amplification refractory mutation system-polymerase chain (ARMS-PCR) of genomic DNA using the following primers: forward outer primers: 5′-TTGTTCCCTTGTTCTTATACCTATTCTGA-3′, reverse outer primers: 5′-CTGTAACAAAATAGGTTCTGACAGCAAC-3′, forward inner primers: 5′-ATTAGAAGATGTTTACATTTTGATGGAAGG-3′, and reverse inner primer: 5′-GTCATTCAAACCATAGTTTAGGTTTGTCTA-3′, which generated 406-bp and 264-bp specific amplicons as fractionated by agarose gel electrophoresis and visualized with ultraviolet light. The 406 bp band corresponds to the *db* allele, while the 264 bp band corresponds to the wild-type (WT) allele.

1.5. Bioinformatics analysis

Glomerular transcriptomic data of health living donors (HLD) or patients with diabetic nephropathy (DN) are publicly available from Nephroseq based on the Ju CKD Glom study [39]. The transcriptomic data were compared between HLD and DN groups to identify differentially expressed genes (DEGs) with a *P* value less than 0.05. The DEGs constituting the curated DN-related gene set "BAELDE_DIABETIC_NEPHROPATHY_UP" were subjected to unsupervised hierarchical cluster analysis together with GSK3β and results displayed by heatmap by using Tbtools [40]. Moreover, to investigate biological pathways associated with GSK3β in diseased glomeruli of DN, the glomerular transcriptomic data were further analyzed by gene set enrichment analysis (GSEA) using the curated DN-related gene set

"BAELDE_DIABETIC_NEPHROPATHY_UP" for specimens with high expression of GSK3β *versus* those with low expression of GSK3β [41]. GSEA was performed by employing GSEA v4.1.0 software (http://software.broadinstitute.org/gsea/index.jsp). In addition, Group-based Prediction System (GPS) 5.0 was used to predict GSK3β phosphorylation consensus motifs in the amino acid sequences of insulin receptor substrate 1 (IRS-1, NCBI Reference Sequence: NP_034700.2) as described previously [42].

1.6. Glomerular isolation

Isolation of glomeruli from mouse kidneys was performed as previously described [16]. Isolated glomeruli were collected and used in the following experiments.

1.7. Western immunoblot analysis and immunoprecipitation

Immortalized mouse podocytes were lysed and isolated mouse glomeruli were homogenized in RIPA buffer supplemented with protease inhibitors (Roche Applied Science, Mannheim, Germany). Besides, NE-PER kit (Thermo Fisher) was used for extracting nuclear fractions. Samples with equal amounts of total protein (20-50 μg per lane) were processed for SDS-PAGE and then immunoblot analysis by using primary and secondary antibodies (The detailed information of applied antibodies was presented in Supplementary Table 1). Immunoprecipitation was performed as previously described [16], and immunoprecipitates were processed for immunoblot analysis for indicated proteins.

1.8. Immunofluorescence staining

Frozen kidney sections or cultured podocytes were fixed with 4% paraformaldehyde (Sigma-Aldrich), permeabilized with 0.25% Triton X-100 in PBS buffer and immersed in 5% BSA in PBS buffer to block the nonspecific background. Sections or cells were incubated with primary antibodies (Supplementary Table 1) overnight and then with secondary antibodies (Supplementary Table 1). Filamentous actin (F-actin) in podocytes was stained by rhodamine-phalloidin (Cytoskeleton Inc, Denver, CO, USA). After counterstaining with 4', 6-diamidino-2-phenylindole (DAPI, Abcam), sections or cells were visualized using a fluorescence microscope (EVOS XL Core Imagine System, Thermo Fisher) or Leica TCS SP5 laser scanning confocal microscope.

1.9. Glucose uptake assay

Glucose uptake by cultured podocytes was measured using the 2-deoxy glucose glucose (2-DG) uptake assay kit (Abcam) according to the manufacturer's instructions. In brief, cells were incubated with the glucose analog 2-DG, and oxidation of the accumulated 2-deoxy-D-Glucose-6-phosphate (2-DG6P) generated NADPH, resulting in oxidation of a substrate, which was measured at ex 535 nm/em 587 nm using Cytation 5 (Agilent Technologies Inc, Santa Clara, CA, USA).

1.10. Detection of reactive oxygen species (ROS) in cells

Intracellular ROS was measured by using the responsive dye 5-(and-6)-chloromethyl-2′,7′-dichlorodihydrofluorescein diacetate (CM-H_2DCFDA; Thermo Fisher), which could be cleaved off the ester groups by intracellular esterases followed by ROS oxidation to generate the intracellular fluorescent DCF derivatives. Briefly, after different treatments, podocytes were loaded with 5 μM CM-H_2DCFDA in a 5% CO_2 humidified incubator for 30 min, followed by microscopic analysis using Invitrogen fluorescence microscope (Thermo Fisher). Then, fluorescence intensity of DCF was estimated by fluorescence spectroscopy with excitation/emission respectively at 485 nm/535 nm using Cytation 5.

Intercellular hydrogen peroxide (H_2O_2) levels were determined using the more reliable phenylboronate-based probe peroxy orange 1 (PO1; Tocris Bioscience, Minneapolis, MN, USA). Briefly, after different treatments, podocytes were loaded with 5 μM PO1 for 30 min. Cells were then processed for microscopic analysis using Invitrogen fluorescence microscope (Thermo Fisher) with Hoechst 33342 (Thermo Fisher) counterstaining. Then, fluorescence intensity of PO1 was estimated by fluorescence spectroscopy with excitation/emission at 543 nm/560 nm using Cytation 5.

As a marker of peroxynitrite-induced oxidative injury, 3-nitrotyrosine (3-NT) was measured by immunoblot analysis of cell lysates using specific antibodies.

1.11. Cell apoptosis detection by terminal deoxynucleotidyl transferase-mediated dUTP nick end labeling (TUNEL) assay

Apoptosis of cultured podocytes was assessed by the TUNEL kit (Promega, Madison, WI, USA) according to the manufacturer's instructions. Briefly, podocytes were fixed with 4% paraformaldehyde and permeabilized with proteinase K solution. Cells were then incubated with equilibration buffer, biotinylated nucleotide mixture, and TdT at 37 °C for 60 min, followed by incubation with streptavidin-HRP solution and with the substrate. After nuclear counterstaining with propidium iodide, cellular apoptosis was examined under a fluorescence microscope (EVOS XL Core Imagine System, Thermo Fisher).

1.12. Senescence-associated β-galactosidase (SA-β-gal) activity staining

The SA-β-gal staining kit (Cell Signaling Technology, Danvers, MA, USA) was used to detect β-galactosidase activity in kidney tissues or cultured podocytes as previously described [22]. Briefly, frozen kidney sections or cells were fixed and incubated with β-galactosidase staining solution containing X-gal at 37 °C. When blue color developed, images were captured using a light microscope after counterstaining of kidney sections with nuclear fast red (Sigma-Aldrich).

1.13. Urinary protein electrophoresis

Equal volumes of spot urine collected from *db/m* and *db/db* mice were analyzed by SDS-PAGE followed by Coomassie Brilliant Blue (Sigma-Aldrich) staining.

1.14. Cell viability assessment by tetrazolium (MTT) assay

The percentage of cell viability was estimated using the MTT assay kit (Sigma-Aldrich) according to the manufacturer's instructions. In brief, after indicated treatments, podocytes were treated with 3-(4,5-diphenylthiazol-2-yl)-2,5-diphenyltetrazolium bromide (0.5 mg/mL) at 37 °C in a 5% CO_2 humidified incubator. After the medium was removed, 200 μL dimethyl sulfoxide (DMSO, Sigma-Aldrich) was added to each well. The absorbance was measured spectrophotometrically at 570 nm with a reference wavelength of 630 nm using Cytation 5.

1.15. Statistical analysis

All *in vitro* experiments were repeated at least three times. For immunoblot analysis, bands were scanned and the integrated pixel density was determined using a densitometer and analyzed by the ImageJ program (version 1.53 National Institutes of Health, Bethesda, MD, USA). Results are expressed as mean ± SD. Statistical analyses were performed using GraphPad Prism 8.0 software (La Jolla, CA, USA). Statistical analysis of data from multiple groups was performed using 1-way ANOVA tests followed by Tukey's tests; data from 2 groups were compared using 2-tailed, unpaired Student's *t*-test. Linear regression analysis was used to test possible associations between 2 parameters. $P < 0.05$ was considered statistically significant.

2. Results

2.1. Exposure to a milieu of type 2 diabetes causes podocyte injury, concomitant with GSK3β hyperactivity

To determine the glomerular expression profile of GSK3β in type 2 DN, a *post-hoc* analysis was conducted based on the publicly available glomerular transcriptomic data derived from the Ju CKD Glom study. Shown in Fig. 1A, glomerular expression of GSK3β was significantly increased in DN group as compared with HLD group. Hierarchical cluster analysis demonstrated that this pattern of alternations in GSK3β expression was similar to that observed in a number of DEGs that constitute the curated DN-related gene set "BAELDE_DIABETIC_NEPHROPATHY_UP", including clusterin (CLU), CD24 molecule (CD24), major histocompatibility complex, class II, DR alpha (HLA-DRA), aldo-keto reductase family 1 member B (AKR1B1), platelet and endothelial cell adhesion molecule 1 (PECAM1), cyclin D1 (CCND1), solute carrier family 22 member 17 (SLC22A17), hemoglobin subunit beta (HBB), and cysteine rich protein 1 (CRIP1). In addition, GSEA revealed that the curated gene set "BAELDE_DIABETIC_NEPHROPATHY_UP" exhibited significant enrichment in high-expression of GSK3β *versus* low-expression of GSK3β in glomeruli in DN patients. To validate these bioinformatic findings, differentiated murine podocytes were exposed to an RPMI 1640-based type 2 diabetic milieu containing high ambient insulin (100 nM) and glucose (25 mM) as well as microinflammation resembled by TNF-α (1 ng/ml) and IL-6 (1 ng/ml) as previously described [43]. As osmotic controls, cells were treated with normal medium containing mannitol (20 mM). After exposure for different times, cells were collected and analyzed. Shown in Fig. 1B by immunofluorescence staining, treatment with the diabetic milieu for 48 h caused striking signs of podocyte injury, featured by morphologic changes and cellular shrinkage as well as reduced expression of the

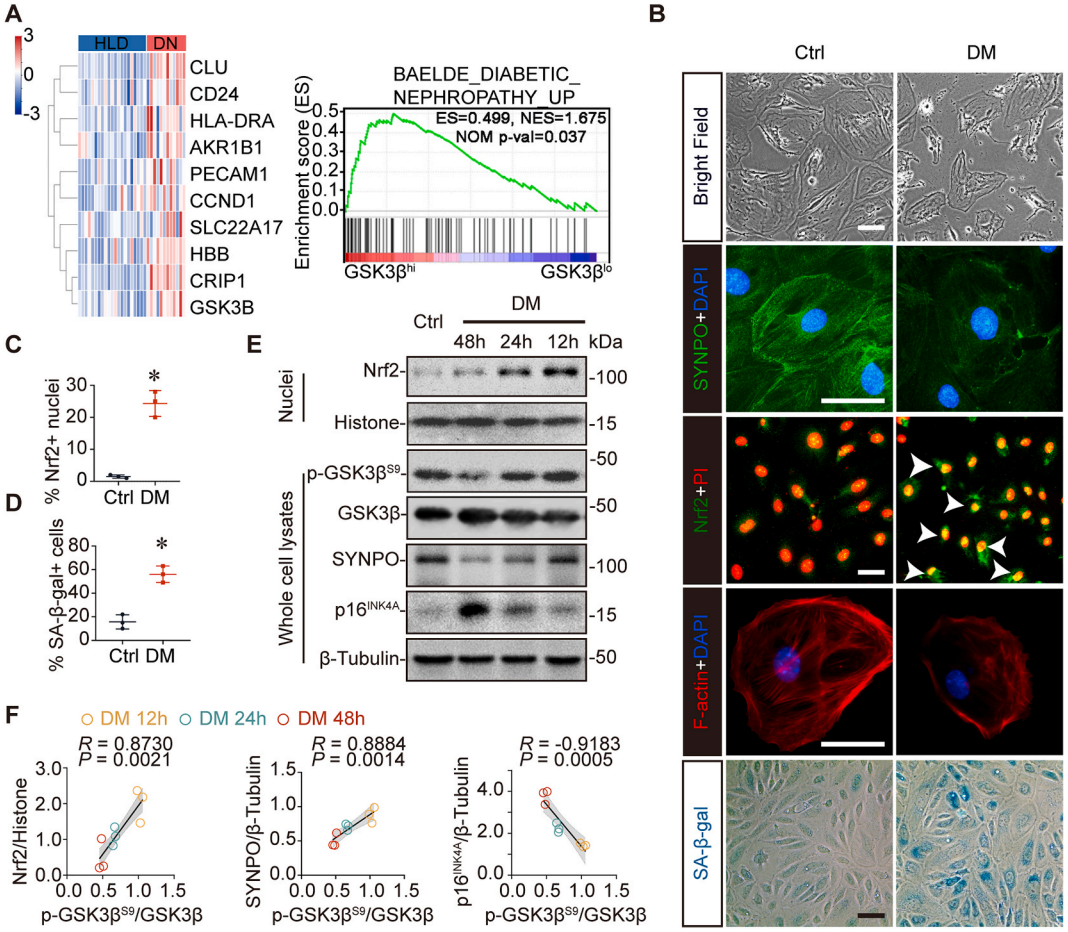

Fig. 1. Diabetic glomerulopathy and podocyte injury in type 2 diabetes is associated with GSK3β hyperactivity.
(A) The mRNA expression data of indicated genes in glomeruli procured from Healthy Living Donors (HLD) (n = 21) and Diabetic Nephropathy (DN) subjects (n = 12) were obtained from the Ju CKD Glom database and then subjected to hierarchical cluster analysis and heat map representation. Color scale represents the relative gene expression value for each gene using $\log_2$ median-centered intensity values. Gene set enrichment analysis (GSEA) of the glomerular transcriptome derived from the Ju CKD Glom study demonstrated that the curated DN-related gene set "BAELDE_DIABETIC_NEPHROPATHY_UP" is enriched in high GSK3β expression phenotype. Enrichment scores (ES), normalized enrichment score (NES) and nominal *P* values are shown. **(B-D)** Murine podocytes were treated with osmotic control (Ctrl) consisting of glucose (5 mM) and mannitol (20 mM) or with type 2 diabetic milieu (DM) consisting of high ambient insulin (100 nM) and high glucose (25 mM), TNF-α (1 ng/ml), and IL-6 (1 ng/ml) for 12, 24, 48 h respectively. **(B)** Representative micrographs of phase contrast light microscopy, immunofluorescence staining for synaptopodin (SYNPO, green) with 4′,6-diamidino-2-phenylindole (DAPI) counterstaining, Nrf2 (green) with propidium iodide (PI) counterstaining, rhodamine-phalloidin staining for F-actin (red) with DAPI counterstaining, and senescence-associated β-galactosidase (SA-β-gal) activity staining (Scale bar, 50 μm). White arrowheads indicate Nrf2 nuclear accumulation. **(C)** Absolute count of the number of the Nrf2-positive podocytes as the percentage of the total number of cells per microscopic field. $^*P < 0.05$ *versus* Ctrl group (n = 3). **(D)** Quantification of the SA-β-gal-positive cells as a percentage of the total number of the cells per microscopic field. $^*P < 0.05$ *versus* Ctrl group (n = 3). **(E)** Representative immunoblot analysis of whole cell lysates and nuclear fractions for indicated proteins. Histone and β-Tubulin served as loading controls. **(F)** Linear regression analysis reveals significant correlations between the relative p-GSK3β^{S9}/GSK3β ratios and the relative expression levels of Nrf2, SYNPO or p16^{INK4A} based on densitometric analysis of immunoblots (n = 3). Spearman's correlation coefficient (*R*) and *P* value are shown. (For interpretation of the references to color in this figure legend, the reader is referred to the Web version of this article.)

homeostatic podocyte marker synaptopodin. Further evidence of podocyte injury and degeneration includes disruption of the integrity of actin cytoskeleton, as shown by phalloidin staining for F-actin. In parallel, significantly more cells in the diabetic milieu group, as opposed to the control group, were positive for SA-β-gal activity staining (Fig. 1B and D), denoting a pro-senescent effect. As a universal cytoprotective machinery harnessed by all mammalian cells for self-protection against any types of stress including diabetic insult, the Nrf2 antioxidant response was apparently triggered in podocyte after exposure to the diabetic milieu, as evidenced by Nrf2 nuclear translocation based on quantification of cells positive for nuclear staining for Nrf2 (Fig. 1B-C). To validate the morphologic findings, whole cell lysates or nuclear fractions were prepared from cells after diabetic insult for different intervals and processed for immunoblot analysis, followed by densitometry. Shown in Fig. 1E-F and Supplementary Fig. 1A-C, exposure to the diabetic milieu time-dependently resulted in increased expression of phosphorylated GSK3β at tyrosine 216 (p-GSK3β^{Y216}) and total GSK3β but reduced expression of the inhibitorily phosphorylated GSK3β at serine 9 (p-GSK3β^{S9}), denoting hyperactivity of the redox-sensitive GSK3β. Although GSK3β phosphorylation at other sites such as Tyr216 may modulate its activity, the primary mechanism of GSK3β activity regulation is phosphorylation of N-terminal serine 9, which can competitively block substrate docking in the substrate binding pocket thereby acting as a dominant negative regulator of GSK3β activity [20]. Therefore, this study focused on changes in the inhibitory phosphorylation of GSK3β at serine 9 in diabetic podocyte injury. Linear regression analysis revealed that the expression ratio of p-GSK3β^{S9}/GSK3β is positively correlated with the expression of synaptopodin, but negatively correlated with expression of p16^{INK4A}, suggesting that GSK3β hyperactivity is associated with diabetes-elicited podocyte degeneration and stress-induced premature senescence. Meanwhile, nuclear accumulation of Nrf2 was increased after exposure to the diabetic milieu. However, nuclear Nrf2 progressively diminished over time and was negatively correlated with the expression ratio of p-GSK3β^{S9}/GSK3β (Fig. 1E-F), implying that GSK3β hyperactivity is associated with a repressed Nrf2 antioxidant response.

2.2. *GSK3β silencing abrogates diabetic podocyte injury by potentiating Nrf2 antioxidant response*

To determine if GSK3β hyperactivity is required for diabetic podocyte injury, podocytes were subjected to siGSK3β or siCtrl before exposure to the diabetic milieu for 24 h. Shown in Fig. 2A, GSK3β silencing as opposed to control-RNAi treatment substantially diminished GSK3β expression. This resulted in preserved expression of synaptopodin upon diabetic insult and reduced expression of the extracellular matrix protein fibronectin (FN), as quantified by densitometry of immunoblots (Fig. 2A-B). In consistency, GSK3β knockdown significantly retained podocyte morphology and the pattern of synaptopodin staining after diabetic insult (Fig. 2C). In addition, diabetic injury caused evident podocyte apoptosis and this effect was apparently abrogated by GSK3β knockdown, as shown by TUNEL staining and absolute counting of TUNEL-positive cells (Fig. 2C-D). Moreover, podocytes with GSK3β knockdown as compared to control cells were found to be less likely positive for SA-β-gal staining upon diabetic injury, denoting an improved senescence (Fig. 2C and E). In support of this, fluorescent immunocytochemistry staining of γH2AX, a molecular marker for DNA double-strand breaks and aging, demonstrated that the formation of γH2AX foci elicited by diabetic insult was significantly mitigated by GSK3β silencing, associated with lessened degenerative changes as shown by improved actin cytoskeleton disarrangement on phalloidin staining (Fig. 2C). The anti-senescent effect of GSK3β knockdown is also supported by the reduced expression of γH2AX and various senescence signaling transducers like p16^{INK4A}, p21, and p53 but increased expression of p-Rb on immunoblot analysis (Fig. 2A-B). Furthermore, the expression of senescence-associated secretory phenotype (SASP) factors such as transforming growth factor-β1 (TGF-β1), insulin like growth factor binding protein 3 (IGFBP3) and plasminogen activator inhibition-1 (PAI-1) was also decreased by GSK3β knockdown in podocytes exposed to the diabetic milieu (Fig. 2A-B).

The above protective effect of GSK3β silencing was associated with enhanced nuclear accumulation of Nrf2, as shown by fluorescent immunocytochemistry staining and by immunoblot analysis of isolated nuclei for Nrf2 (Fig. 2F-G and I-J). Consequently, expression of Nrf2 target antioxidant molecules, including heme oxygenase-1 (HO-1) and NAD(P)H quinone dehydrogenase 1 (NQO1) were potentiated by GSK3β knockdown in podocytes exposed to the diabetic milieu (Fig. 2I-J). As enzymatic antioxidants, HO-1 and NQO1 are known to eliminate ROS [44–46]. Indeed, the above changes induced by GSK3β knockdown were associated with reduced production of ROS, as shown by diminished DCF staining (Fig. 2F). Although DCF fluorescence is widely used to detect ROS, recent studies suggest that this technique lacks specificity for individual oxidants and may be unreliable due to a number of drawbacks, including the unspecificity and the generation of radicals it is purported to measure [47]. In contrast, PO1 is a deprotection reaction-based probe that fluoresces upon H_2O_2-specific removal of a boronate group rather than non-specific oxidation and is specifically sensitive to H_2O_2 among ROS [48]. As such, to complement the DCF findings, PO1 staining was further carried out to specifically determine intracellular H_2O_2 levels. Shown in Fig. 2F and H, PO1 staining in podocytes exposed to diabetic insult was mitigated by GSK3β knockdown, denoting a reduced production of H_2O_2. Evidence suggests that despite a high selectivity for H_2O_2, PO1, to a much lesser extent, shows relatively small fluorescence enhancement in response to peroxynitrite [49]. To confirm if a change in peroxynitrite also occurs, 3-NT, a marker of peroxynitrite-induced oxidative injury, was measured by immunoblot analysis. Shown in Fig. 2I-J, GSK3β knockdown markedly suppressed the levels of proteins modified by nitration in podocytes exposed to diabetic insult, implying a possible reduction in peroxynitrite. Oxidative stress is known to cause inflammation. In parallel with the changes in ROS, GSK3β silencing, as opposed to control-RNAi treatment, diminished the expression of pro-inflammatory cytokines such as MCP-1 in podocytes exposed to the type 2 diabetic milieu (Supplementary Fig. 2A-B).

To ascertain if the reinforced Nrf2 antioxidant response mediates the protective effect of GSK3β knockdown against diabetic podocyte injury, a separate group of GSK3β-silenced cells were simultaneously treated with Trig, a selective inhibitor of Nrf2. Despite a comparable magnitude of GSK3β knockdown, Trig treatment counteracted Nrf2 nuclear accumulation, abolished the increased expression of HO-1 and NQO1, and restored H_2O_2 production and levels of protein nitration as well as MCP-1 levels, denoting an effective Nrf2 blocking activity (Fig. 2F-J and Supplementary Fig. 2A-B). This resulted in the abrogation of the synaptopodin-preserving effect of GSK3β silencing, as shown by immunoblot analysis and fluorescent immunocytochemistry staining (Fig. 2A-C), and overrode the anti-apoptotic action, as revealed by TUNEL staining (Fig. 2C-D). Moreover, Trig treatment abolished the anti-senescent effect of GSK3β knockdown, as shown by the lessened reduction in SA-β-gal activity staining, γH2AX foci formation, the expression of p16^{INK4A}, p21, and p53, and the expression of the SASP factors, whereas diminished induction of p-Rb expression (Fig. 2A-C and E). This was associated with a mitigated improvement in podocyte degeneration, marked by actin cytoskeleton derangement (Fig. 2C).

2.3. *Ectopic expression of the constitutively active GSK3β exacerbates diabetic podocyte injury via suppressing Nrf2 antioxidant response*

To determine whether GSK3β hyperactivity is sufficient to cause diabetic podocyte injury, podocytes were transfected with EV or a vector encoding the HA-tagged constitutively active mutant of GSK3β (S9A), in which the serine 9 amino acid residual was replaced by alanine, followed by exposure to the type 2 diabetic milieu for 48 h. As shown in Fig. 3A and D, immunofluorescent staining for HA and immunoblot

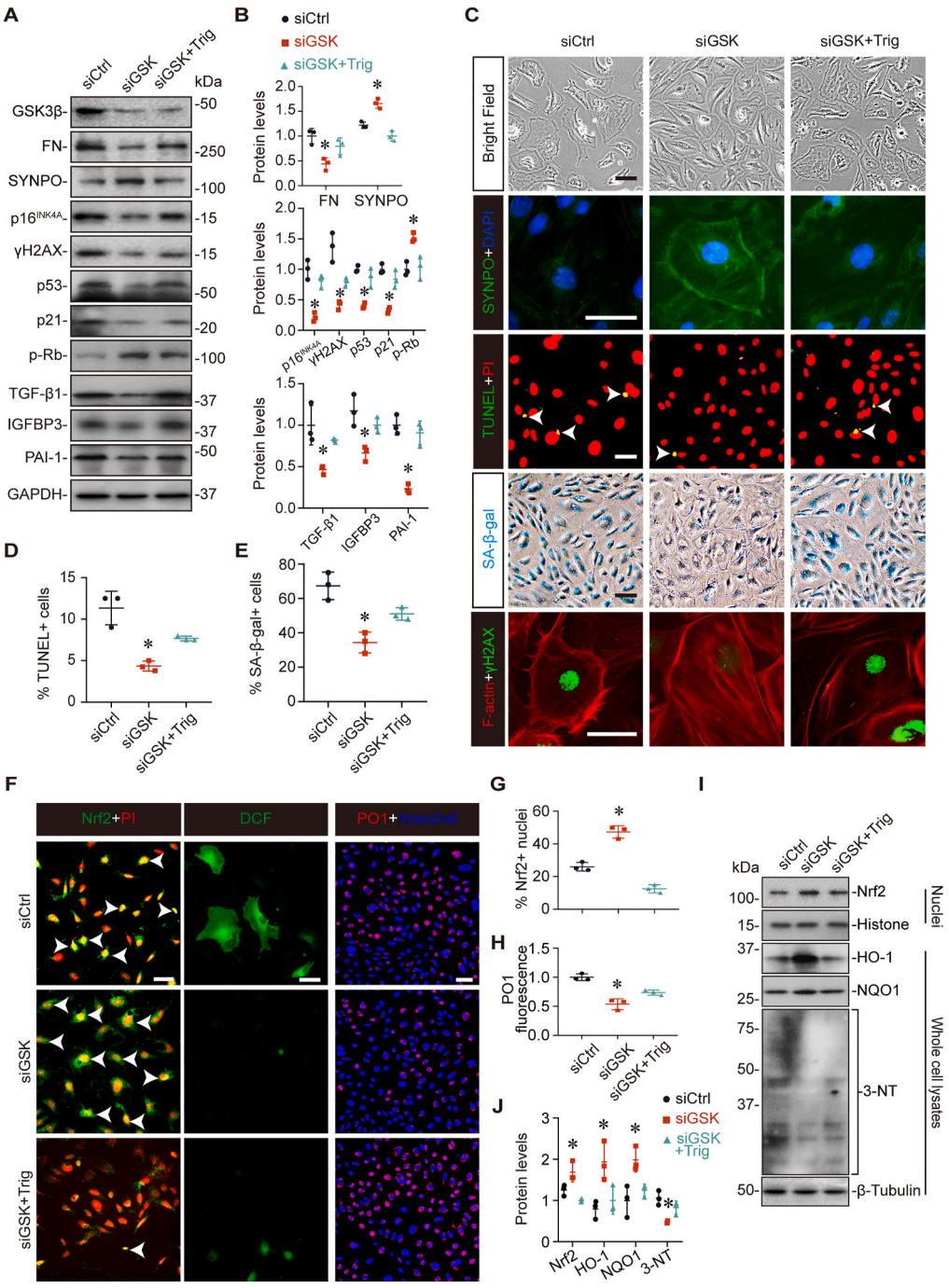

Fig. 2. Knockdown of GSK3β protects against senescence and injury in podocytes upon diabetic insults by reinforcing Nrf2-mediated antioxidant response. Murine podocytes expressing specific siRNA against GSK3β (siGSK) or control siRNA (siCtrl) were stimulated with the type 2 DM as described in Fig. 1B in the presence or absence of trigonelline (Trig, 30 μM) for 48 h. **(A)** Representative immunoblot analysis of whole cell lysates for indicated proteins. GAPDH served as a loading control. **(B)** Densitometric analysis of the expression levels of the indicated proteins, presented as relative levels normalized to GAPDH based on immunoblot analysis. *$P < 0.05$ *versus* other groups for the same protein (n = 3). **(C)** Representative micrographs of light microscopy, immunofluorescence staining for SYNPO (green) with DAPI counterstaining, γH2AX (green) with rhodamine-phalloidin counterstaining for F-actin, the terminal deoxynucleotidyl transferase-mediated dUTP nick end labeling (TUNEL) staining with PI counterstaining and SA-β-gal activity staining (Scale bar, 50 μm). White arrowheads indicate TUNEL-positive cells. **(D)** Absolute count of the number of the TUNEL staining-positive podocyte as a percentage of the total number of cells per microscopic field. *$P < 0.05$ *versus* other groups (n = 3). **(E)** Quantification of the SA-β-gal-positive cells as a percentage of the total number of the cells per microscopic field. *$P < 0.05$ *versus* other groups (n = 3). **(F)** Representative micrographs of immunofluorescence staining for Nrf2 (green) with PI counterstaining, 5-(and-6)-chloromethyl-2′,7′-dichlorodihydro-fluorescein diacetate (DCF) staining, and peroxy orange 1 (PO1, red) with Hoechst 33342 counterstaining (Scale bar, 50 μm). White arrowheads indicate Nrf2 nuclear accumulation. **(G)** Absolute count of the number of the Nrf2-positive podocytes as a percentage of the total number of cells per microscopic field. *$P < 0.05$ *versus* other groups (n = 3). **(H)** Relative fluorescence intensity of PO1 staining. *$P < 0.05$ *versus* other groups (n = 3). **(I)** Representative immunoblot analysis of whole cell lysates and nuclear fractions for indicated proteins. Histone and β-Tubulin served as loading controls. **(J)** Densitometric analysis of the expression levels of indicated proteins, presented as relative levels normalized to Histone (for Nrf2) or β-Tubulin (for other proteins) based on immunoblot analysis. *$P < 0.05$ *versus* other groups (n = 3). (For interpretation of the references to color in this figure legend, the reader is referred to the Web version of this article.)

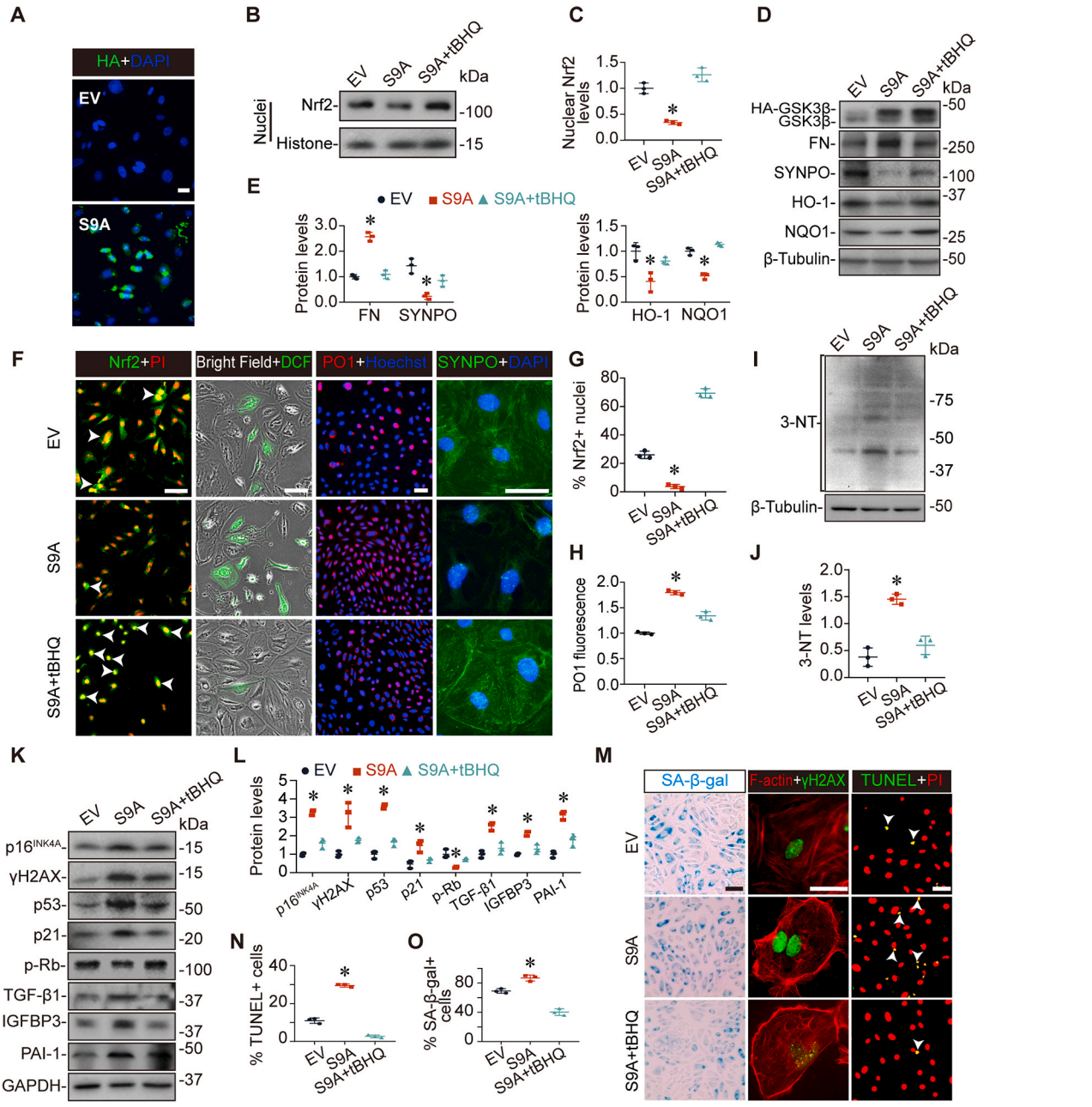

Fig. 3. GSK3β represses the antioxidant defense through inhibiting the expression of Nrf2 in podocytes exposed to the type 2 diabetic milieu.
Murine podocytes were transiently transfected with a control plasmid empty vector (EV), or a plasmid encoding the hemagglutinin (HA)-conjugated dominant-constitutively active mutant of GSK3β (S9A) for 24 h. After transfection, cells were cultured in the type 2 DM as described in Fig. 1B in the presence or absence of tert-butylhydroquinone (tBHQ, 20 μM) for 48 h. **(A)** After transfection, cells were subjected to immunofluorescent staining for HA (green) with DAPI counterstaining for nuclei, which revealed a transfection efficiency of approximately 80% (Scale bar, 50 μm). **(B)** Representative immunoblot analysis of nuclear fractions for Nrf2. Histone served as a loading control. **(C)** Densitometric analysis of the expression levels of Nrf2 protein, presented as relative levels normalized to Histone based on immunoblot analysis. *$P < 0.05$ *versus* other groups (n = 3). **(D)** Representative immunoblot analysis of whole cell lysates for indicated proteins. β-Tubulin served as a loading control. **(E)** Densitometric analysis of the expression levels of the indicated proteins, presented as relative levels normalized to β-Tubulin based on immunoblot analysis. *$P < 0.05$ *versus* other groups for the same protein (n = 3). **(F)** Representative micrographs of Nrf2 (green) staining with PI counterstaining, light microscopy merged with DCF staining, PO1 staining (red) with Hoechst 33342 counterstaining, and SYNPO (green) immunofluorescence staining with DAPI counterstaining (Scale bar, 50 μm). White arrowheads indicate Nrf2 nuclear accumulation. **(G)** Absolute count of the number of the Nrf2-positive podocytes presented as the percentage of the total number of cells per microscopic field. *$P < 0.05$ *versus* other groups (n = 3). **(H)** Relative fluorescence intensity of PO1 staining. *$P < 0.05$ *versus* other groups (n = 3). **(I)** Representative immunoblot analysis of whole cell lysates for 3-NT. β-Tubulin served as a loading control. **(J)** Densitometric analysis of the levels of 3-NT, presented as relative levels normalized to β-Tubulin based on immunoblot analysis. *$P < 0.05$ *versus* other groups (n = 3). **(K)** Representative immunoblot analysis of whole cell lysates for indicated proteins. GAPDH served as a loading control. **(L)** Densitometric analysis of the expression levels of the indicated proteins, presented as relative levels normalized to GAPDH based on immunoblot analysis. *$P < 0.05$ *versus* other groups for the same protein (n = 3). **(M)** Representative micrographs of SA-β-gal activity staining, immunofluorescence staining for γH2AX (green) with rhodamine-phalloidin counterstaining for F-actin, and TUNEL staining with PI counterstaining (Scale bar, 50 μm). White arrowheads indicate TUNEL staining positive cells. **(N)** Absolute count of the number of the TUNEL staining-positive podocytes presented as the percentage of the total number of cells per microscopic field. *$P < 0.05$ *versus* other groups (n = 3). **(O)** Quantification of the SA-β-gal-positive cells as the percentage of the total number of the cells per microscopic field. *$P < 0.05$ *versus* other groups (n = 3). (For interpretation of the references to color in this figure legend, the reader is referred to the Web version of this article.)

analysis confirmed a satisfactory transfection efficiency of podocytes with plasmids encoding S9A. Forced expression of S9A worsened diabetic podocyte injury, as evidenced by amplified expression of fibronectin and reduced expression of synaptopodin on immunoblot analysis and fluorescent immunocytochemistry staining (Fig. 3D-F). In addition, shown by TUNEL staining, diabetic injury-induced apoptosis was promoted by in S9A-expressing podocytes, as compared to those expressing EV (Fig. 3M-N). Moreover, ectopic expression of S9A enhanced the diabetic injury-induced expression of γH2AX and various senescence signaling transducers like p16^{INK4A}, p21, and p53, but repressed the expression of p-Rb on immunoblot analysis (Fig. 3K-L). This was associated with increased formation of γH2AX foci and more cells positive for SA-β-gal staining (Fig. 3M and O), indicative of a promoted cellular senescence. In agreement, upon exposure to diabetic milieu, S9A-expressing podocytes, as opposed to EV-transfected cells, produced higher levels of SASP factors such as TGF-β1, IGFBP3, and PAI-1, and exhibited more severe signs of cellular degeneration, marked by actin cytoskeleton disorganization (Fig. 3K-M).

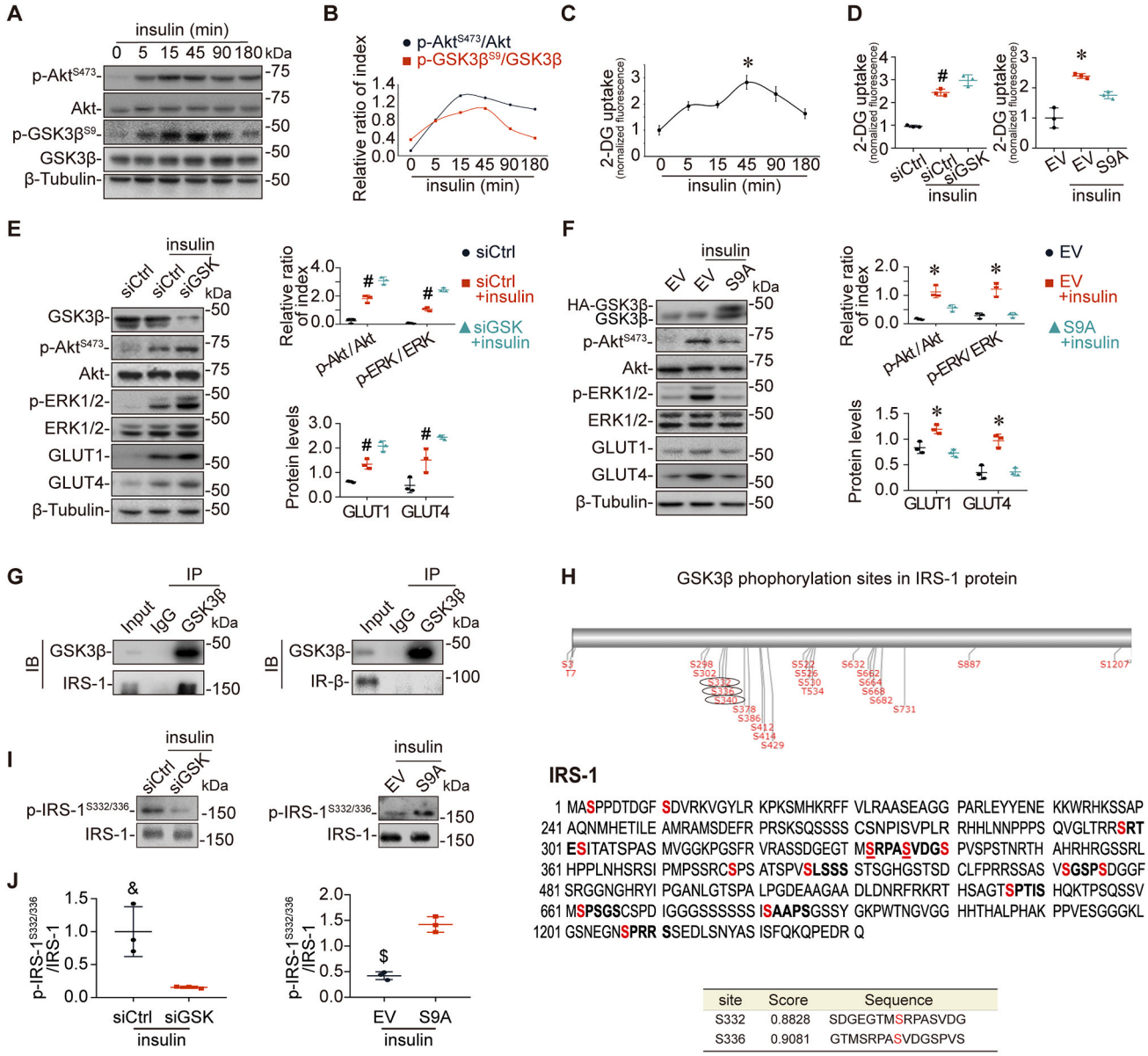

Fig. 4. Over-activation of GSK3β desensitizes insulin signaling through regulating the phosphorylation of IRS-1 in podocytes.
(A) Murine podocytes were treated with RMPI 1640 medium containing insulin (100 nM) for different times (5min, 15min, 45min, 90min, 180min) respectively. Representative immunoblot analysis of whole cell lysates for indicated proteins. β-Tubulin served as a loading control. **(B)** Densitometric analysis of the expression levels of p-Akt^{S473}/Akt and p-GSKβ^{S9}/GSK3β at different time points. **(C)** Quantitation of 2-deoxyglucose (2-DG) uptake after treatment with insulin (100 nM) for indicated times. *$P < 0.05$ *versus* other time points (n = 3). **(D)** Quantitation of 2-DG uptake after insulin (100 nM) for 45min in cells with different transfections. $^{\#}$, *$P < 0.05$ *versus* other groups (n = 3). **(E-F)** Representative immunoblot analysis of whole cell lysates for indicated proteins. β-Tubulin served as a loading control. Densitometric analysis of the relative expression levels of p-Akt^{S473}/Akt (p-Akt/Akt), p-ERK1/2/ERK1/2 (p-ERK/ERK). Expressions of GLUT1 and GLUT4 were presented as relative levels normalized to β-Tubulin based on immunoblot analysis. $^{\#}$, *$P < 0.05$ *versus* other groups for the same protein (n = 3). **(G)** Lysates of cultured murine podocytes were processed for immunoprecipitation (IP) by using an anti-GSK3β antibody or IgG isotype control (IgG), followed by immunoblot analysis (IB) of the immunoprecipitates for GSK3β, IRS-1 and IR-β in parallel with input controls. **(H)** *In silico* analysis demonstrated that serine/threonine residues of IRS-1 reside in the consensus motifs for phosphorylation by GSK3β. The serines with high prediction scores for GSK3β consensus motifs are marked with black circles. **(I)** Representative immunoblot analysis of whole cell lysates for indicated proteins. **(J)** Densitometric analysis of the expression levels of p-IRS-1$^{S332/336}$/IRS-1. $^{\&}$, $^{\$}P < 0.05$ *versus* siGSK or S9A group (n = 3).

In parallel with all the above detrimental effects, ectopic expression of S9A also blunted the Nrf2 antioxidant response to diabetic injury, as evidenced by enhanced H_2O_2 production and protein tyrosine nitration (Fig. 3F and H-J), reduced induction of Nrf2 target molecules like HO-1 and NQO1 and lessened nuclear accumulation of Nrf2 on immunoblot analysis or fluorescent immunocytochemistry staining (Fig. 3B-G). This was associated with an increased MCP-1 level in S9A-expressing podocytes. (Supplementary Fig. 2C-D).

To test if the S9A-worsened diabetic podocyte injury is attributable to the dampened Nrf2 antioxidant response, a separate group S9A-expressing cells were treated with tBHQ, a potent activator of Nrf2. Consistent with its Nrf2 activating activity, tBHQ treatment significantly increased Nrf2 nuclear translocation, upregulated the expression of HO-1 and NQO1, and attenuated the generation of H_2O_2 and levels of protein nitration as well as MCP-1 production in S9A-expressing cells upon exposure to the diabetic milieu, resulting in an improved podocyte injury as evidenced by preserved expression of synaptopodin, reduced expression of fibronectin as well as diminished apoptosis shown by TUNEL staining (Fig. 3B-J and M-N, Supplementary Fig. 2C-D). Meanwhile, tBHQ also averted the S9A promoted podocyte senescence, as shown by the lessened induction of the expression of $p16^{INK4A}$, p21, p53, and the SASP factors, mitigated increase in γH2AX foci formation and SA-β-gal staining, whereas restored expression of p-Rb (Fig. 3K-M and O). This was associated with an improvement in podocyte degeneration, marked by actin cytoskeleton derangement (Fig. 3M).

2.4. *GSK3β hyperactivity impairs the signaling activity of insulin pathway in glomerular podocytes*

In addition to being a convergent point for multiple podocytopathic pathways, GSK3β is a key mediator of the insulin pathway and dictates glycogen biogenesis [20,50]. Emerging evidence suggests that insulin signaling in kidney cells, in particular podocytes, plays a critical role in maintaining kidney homeostasis independent of blood glucose levels [51,52]. To determine whether and how GSK3β is involved in the regulation of insulin signaling in podocytes, molecular dissection of the podocyte insulin pathway was performed. In response to insulin stimulation, signaling transducers downstream of the insulin pathway, including Akt and GSK3β, were phosphorylated in a time-dependent fashion in podocytes, as shown by immunoblot analysis (Fig. 4A-B). In parallel, insulin stimulation time-dependently increased podocyte uptake of glucose, which peaked at 45 min and decreased thereafter (Fig. 4C). GSK3β silencing sensitized the insulin signaling, marked by a potentiated induction of phosphorylation of Akt and ERK1/2 (Fig. 4E). This was associated with an enhanced glucose uptake and insulin-induced expression of glucose transporter (GLUT)1 and GLUT4 (Fig. 4D-E). In contrast, in cells expressing S9A, GSK3β hyperactivity de-sensitized the insulin signaling, marked by a blunted induction of phosphorylation of Akt and ERK1/2 by insulin (Fig. 4F). This was associated with a dampened induction of GLUT1 and GLUT4 expression, concomitant with a lessened increase in glucose uptake (Fig. 4D and F).

To decipher the molecular basis underlying the GSK3β regulation of the insulin signaling, we next examined possible interactions between GSK3β and diverse signaling transducers proximal to the insulin pathway, including insulin receptor (IR)-β and IRS-1. Immunoprecipitation was carried out and demonstrated that GSK3β apparently co-precipitated with IRS-1 but not IR-β, suggesting that GSK3β might physically interacts with IRS-1 (Fig. 4G). A growing body of evidence suggests that IRS-1 undergoes posttranslational regulation, including phosphorylation [53]. In addition, as a ubiquitously expressed serine/threonine kinase, GSK3β is known to catalyze the phosphorylation of a number of substrate proteins [20]. To further test if physical interaction between GSK3β and IRS-1 causes a corollary effect on IRS-1 phosphorylation, the amino acid sequence of mouse IRS-1 was subjected to the computational active site analysis for putative consensus phosphorylation motifs (S/T-xxx-S/T) for GSK3β. *In silico* analysis indicated that a number of residues in IRS-1 including serine 332, 336 and 340 reside in the consensus motifs for phosphorylation by GSK3β with statistically significant prediction scores. Among these residues, serine 332 as well as the associated serine 336 were located to a same GSK3β substrate motif and had the highest prediction score, inferring a high-confidence match to GSK3β phosphorylation motif and that $IRS\text{-}1^{S332}$ is a putative cognate substrate for GSK3β (Fig. 4H). Of note, serine 332 of IRS-1 has been shown to negatively regulate IRS-1 activity and target IRS-1 for proteasomal degradation [54]. To validate the findings of in silico analysis, the effect of manipulation of GSK3β activity on phosphorylation of IRS-1 at serine 332 was examined. Shown in Fig. 4I-J, insulin-induced phosphorylation of IRS-1 at serine 332 was markedly suppressed by GSK3β knockdown but was significantly elevated in S9A-expressing cells with GSK3β hyperactivity. These data suggest that GSK3β modulates the insulin signaling in podocytes *via*, at least in part, a direct regulatory effect on the IRS-1 activity that is achieved by directing the phosphorylation of IRS-1 at serine 332.

2.5. *Pharmacological targeting of GSK3β by a small molecule inhibitor protects against diabetic injury and re-sensitizes insulin signaling in glomerular podocytes*

A number of small molecule inhibitors have been developed and synthesized with a high selectivity on GSK3β [55]. TDG is the first clinically relevant highly selective small molecule inhibitor of GSK3β that has completed Phase II clinical trial and proven safe and well tolerated [30]. To test the effect of pharmacological targeting of GSK3β on diabetic podocyte injury, TDG was used to treat podocytes upon exposure to the diabetic milieu. As expected, TDG suppressed the activity of GSK3β, marked by enhanced inhibitory phosphorylation of GSK3β at serine 9 (Fig. 5A). This was associated with a dose-dependent improvement of cell viability as shown by the MTT assay (Fig. 5B). The protective effect of TDG coincided with a reinforced Nrf2 antioxidant response and reduced production of peroxynitrite as revealed by increased nuclear translocation of Nrf2 and reduced levels of proteins modified by nitration (Fig. 5C-D and G-H). In parallel, diabetic insult-induced podocyte senescence was abrogated by TDG co-treatment, as evidenced by a considerable reduction in cells positive for SA-β-gal staining and in γH2AX foci formation (Fig. 5E-F). This was associated with an improvement in podocyte degeneration, marked by actin cytoskeleton derangement (Fig. 5E). In addition, TDG treatment counteracted the diabetic insult-induced hyperphosphorylation of IRS-1 at serine 332 in podocytes, indicative of a re-sensitized insulin signaling (Fig. 5C-D).

2.6. *The redox-sensitive GSK3β is hyperactive in glomerular podocytes in db/db mice with DKD, associated with enhanced IRS-1 phosphorylation, impaired Nrf2 response and premature senescence*

To verify the role of GSK3β in podocyte injury in DKD *in vivo*, diabetic *db/db* mice were examined along with nondiabetic *db/m* control littermates. The obese phenotype in conjunction with coat color and ARMS-PCR-based genotyping distinguished *db/db* mice from WT and *db/m* littermates as shown in Fig. 6A-B. At 16 weeks of age, *db/db* mice, as opposed to control mice, developed prominent DN and diabetic podocytopathy, as evidenced by abundant albuminuria on urine protein electrophoresis (Fig. 6C) as well as loss of homeostatic podocyte markers such as synaptopodin on fluorescent immunohistochemistry staining (Fig. 6D). This coincided with reduced expression of the inhibitorily phosphorylated GSK3β at serine 9 in synaptopodin-positive glomerular podocytes, denoting GSK3β hyperactivity (Fig. 6D). In addition, dual-color fluorescent immunohistochemistry staining for Nrf2 and wilms' tumor 1 (WT-1) was employed to detect podocyte-specific Nrf2 antioxidant response, marked by nuclear translocation of Nrf2 to WT-1 positive podocyte nuclei (Fig. 6D), followed by absolute counting of glomerular cells positive for WT-1 and those positive for both WT-1 and

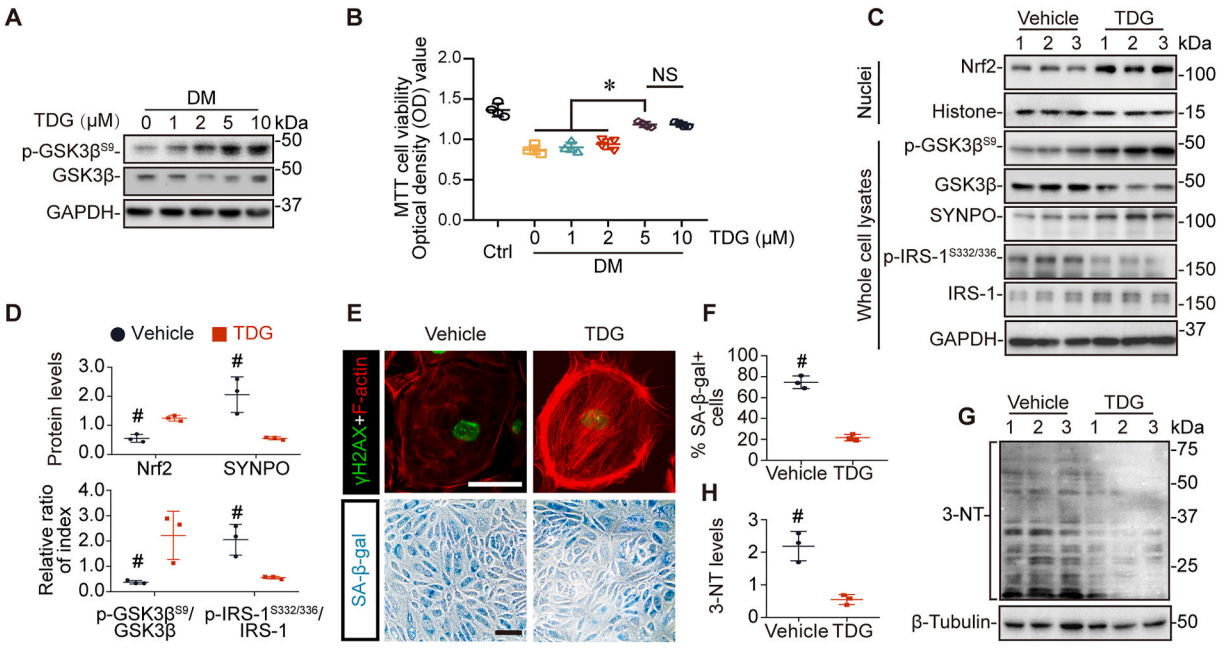

Fig. 5. Tideglusib, an inhibitor of GSK3β, re-sensitizes insulin signaling, reinstates Nrf2 antioxidant response and alleviates podocyte injury and senescence upon diabetic insult.

(A) Murine podocytes were cultured in type 2 DM as described in Fig. 1B in the presence of tideglusib (TDG) at varying concentrations for 48 h. Representative immunoblot analysis of whole cell lysates for indicated proteins including p-GSK3β^{S9} and GSK3β. GAPDH served as a loading control. **(B)** Podocyte viability was determined by MTT assay after treatment with Ctrl as described in Fig. 1 and type 2 DM in the presence of TDG at varying concentrations for 48 h $^{*}P < 0.05$; NS, non-significance (n = 4). **(C)** Representative immunoblot analysis of whole cell lysates and nuclear fractions for indicated proteins. Histone and GAPDH served as loading controls. **(D)** Densitometric analysis of the expression levels of the indicated proteins, presented as relative levels of Nrf2 normalized to Histone, SYNPO normalized to GAPDH, or relative expression ratios of p-GSKβ^{S9}/GSK3β and p-IRS-1$^{S332/336}$/IRS-1 based on immunoblot analysis. $^{\#}P < 0.05$ *versus* TDG group for the same protein (n = 3). **(E)** Representative micrographs of immunofluorescence staining for γH2AX (green) with rhodamine-phalloidin counterstaining for F-actin, and SA-β-gal activity staining (Scale bar, 50 μm). **(F)** Quantification of the SA-β-gal-positive cells as the percentage of the total number of the cells per microscopic field. $^{\#}P < 0.05$ *versus* TDG group (n = 3). **(G)** Representative immunoblot analysis of whole cell lysates for 3-NT. β-Tubulin served as a loading control. **(H)** Densitometric analysis of the levels of 3-NT, presented as relative levels normalized to β-Tubulin based on immunoblot analysis respectively. $^{\#}P < 0.05$ *versus* other groups (n = 3). (For interpretation of the references to color in this figure legend, the reader is referred to the Web version of this article.)

Nrf2 per glomerular cross section (Fig. 6E-F). Since diabetic kidney disease in the diabetic *db/db* mice is known to be associated with podocytopenia [56], podocytes in the *db/db* group, marked by glomerular cells positive for WT-1 staining, were, as expected, significantly fewer than those in the control *db/m* group. In contrast, the number of Nrf2-positive podocytes as well as the percentage of podocytes positive for Nrf2 per glomerular cross section was substantially greater in the diabetic *db/db* group than in the control *db/m* group, suggesting that diabetic kidney injury is associated with Nrf2 antioxidant self-defense in glomerular podocytes. This finding was further verified by immunoblot analysis of nuclei extracted from isolated glomerular, which demonstrated a variably increased nuclear accumulation of Nrf2 in *db/db* mice, indicative of a spontaneous Nrf2 antioxidant response of variable magnitude to diabetic insult (Fig. 6G). Consistent with our finding, previous studies [57,58] demonstrated that human DN is also associated with increased nuclear accumulation of Nrf2 in podocytes. Moreover, glomerular expression of phosphorylated IRS-1 at serine 332 was variably augmented in glomerular podocytes, as shown by fluorescent immunohistochemistry staining in synaptopodin-positive glomerular podocytes followed by immunoblot analysis of isolated glomeruli (Fig. 6D and H). Furthermore, glomerular staining for the senescence marker SA-β-gal activity was variably increased in diabetic mice as shown in Fig. 6D. Linear regression analysis revealed that the expression ratio of p-GSK3β^{S9}/GSK3β was negatively correlated with the number of WT-1 positive cells per glomerular cross section but positively correlated with the number of SA-β-gal positive foci per glomerular cross section in *db/db* mice, suggesting that GSK3β hyperactivity is associated with podocyte injury and senescence in DN (Fig. 6I). Besides, the expression ratio of p-GSK3β^{S9}/GSK3β was negatively correlated with the expression of p-IRS-1 at serine 332 in glomeruli, denoting a desensitized insulin signaling (Fig. 6I). Finally, a positive correlation between the expression ratio of p-GSK3β^{S9}/GSK3β and the expression of nuclear Nrf2, coupled with a negative correlation between the expression ratio of p-GSK3β^{S9}/GSK3β and the levels of proteins modified by nitration in glomeruli in *db/db* mice (Fig. 6I), suggests that GSK3β hyperactivity is associated with an impaired Nrf2 antioxidant response and augmented oxidative stress.

3. Discussion

DKD is a common and serious complication of diabetes, and has become a major contributor to the increasing burden of chronic kidney disease worldwide due to the growing diabetes pandemic [1,3]. Diabetic podocyte injury underlies the progression of albuminuria and glomerulopathy [15]. The present study demonstrated that the redox-sensitive GSK3β is a key mediator driving podocyte injury in type 2 DKD [22,28]. To the best of our knowledge, this study is the first to demonstrate the pivotal role of GSK3β in regulating podocyte injury in type 2 diabetes.

The contribution of GSK3β signaling to diabetes-related pathology in other tissues like muscle [59], fat [60] and heart [61] has been well defined and established before. However, the role of GSK3β in DKD has been extremely controversial based on very few studies that involved only the streptozotocin (STZ)-elicited type 1 diabetes models and relied solely on either chemical inhibitors or activators with specificity concerns [31,62,63]. For instance, in rats with STZ-elicited diabetes, Lin et al. [62] found that inhibition of GSK3β by an ATP-competitive inhibitor 6-Bromo indirubin-3′-oxime (BIO) attenuated proteinuria and glomerular lesions of DN in the absence of correction of hyperglycemia,

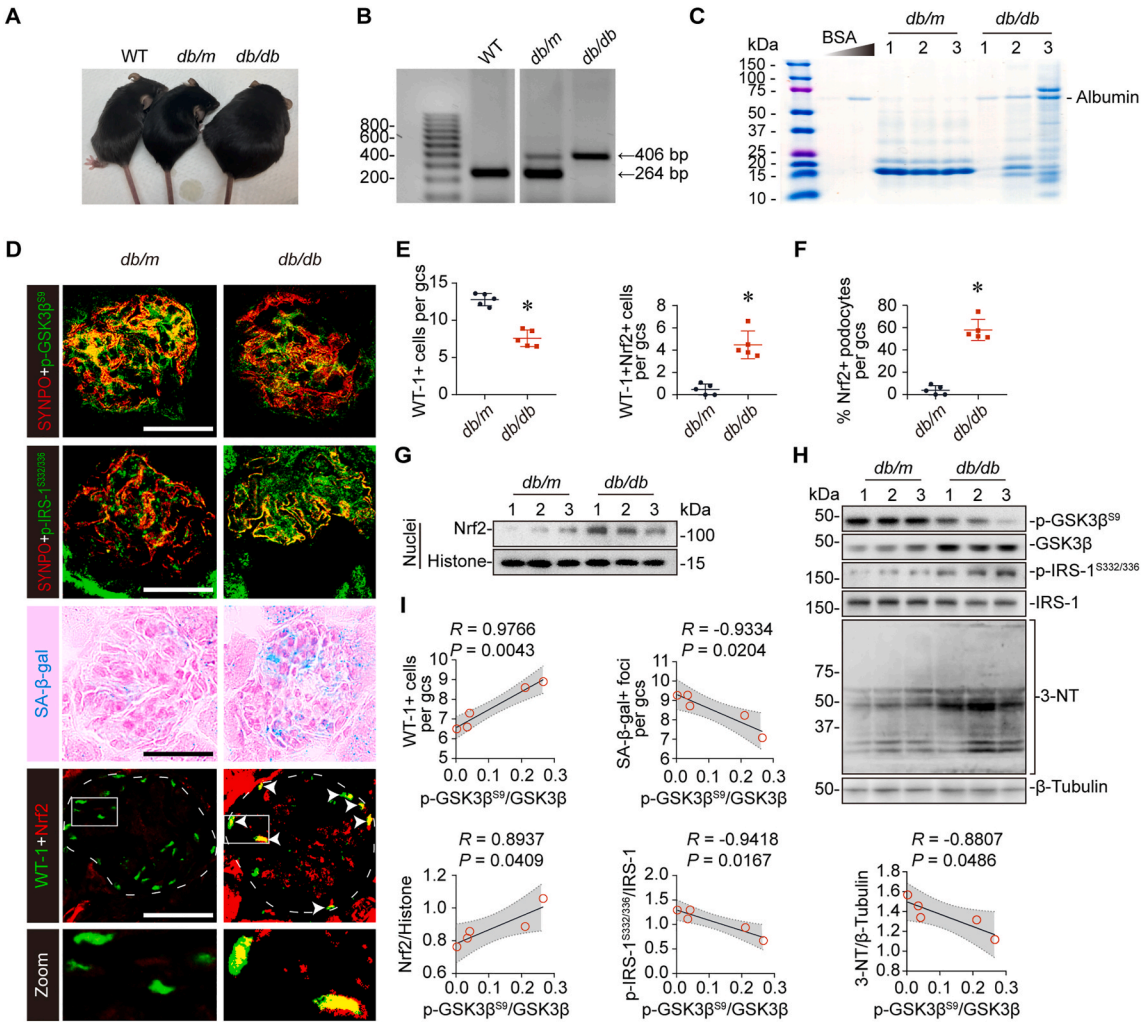

Fig. 6. GSK3β hyperactivity is evident in glomerular podocytes in *db/db* mice with type 2 diabetic nephropathy, associated with podocyte injury, impaired antioxidant response, premature senescence and IRS-1 hyperphosphorylation.

(A) Representative image of the gross appearance of a litter of WT, *db/m* and *db/db* mice. **(B)** Representative agarose gel electrophoresis showing genotyping of indicated mice. **(C)** Equal aliquots (20 μL) of spot urine were subjected to SDS-PAGE followed by Coomassie brilliant blue staining. Bovine serum albumin (BSA, 0.1 and 1.5 μg) were used as standard controls. **(D)** Frozen kidney sections were processed for dual-color immunofluorescence staining for p-GSK3β^{S9} (green) and SYNPO (red), p-IRS-1$^{S332/336}$ (green) and SYNPO (red), WT-1 (green) and Nrf2 (red), and SA-β-gal activity staining (Scale bar, 50 μm). White arrowheads indicate representative glomerular podocytes positive for both Nrf2 and WT-1 staining. In the zoomed views of the boxed areas, Nrf2 colocalized with WT-1 positive podocyte nuclei in *db/db* mice. **(E)** Glomerular cells positive for WT-1 staining or for both WT-1 and Nrf2 staining per glomerulus cross section (gcs) were quantified by absolute counting, and a mean value was calculated and presented using the values obtained in 10 glomerular cross sections per animal. *$P < 0.05$ *versus db/m* groups (n = 5). **(F)** Percentage (%) of podocyte positive for Nrf2 staining per gcs was calculated based on data in **(E)**. *$P < 0.05$ *versus db/m* groups (n = 5). **(G)** Representative immunoblot analysis of nuclear fractions of isolated glomeruli for indicated proteins. Histone served as a loading control. **(H)** Representative immunoblot analysis of whole lysates of isolated glomeruli for indicated proteins. β-Tubulin served as loading controls. **(I)** Linear regression analysis reveals significant correlations between relative p-GSK3β^{S9}/GSK3β ratios and the average WT-1 positive cells or the average SA-β-gal positive foci per glomerular cross section, the relative expression of nuclear Nrf2, the expression ratios of p-IRS-1$^{S332/336}$/IRS-1, or the relative levels of 3-NT based on densitometric analysis of immunoblots from *db/db* mice (n = 5). Spearman's correlation coefficient (*R*) and *P* value are shown. (For interpretation of the references to color in this figure legend, the reader is referred to the Web version of this article.)

denoting a detrimental role of GSK3β in DN. In consistency, Paeng et al. [31] made similar findings by using BIO also in STZ-injured rats, and found that BIO treatment attenuated urine albumin excretion. In stark contrast, Mariappan et al. [64] demonstrated that activation of GSK3β ameliorated diabetes-induced kidney injury. They treated mice with STZ-induced diabetes with sodium nitroprusside, a nitric oxide donor that is able to activate GSK3β, and found that albuminuria, kidney hypertrophy and extracellular matrix expansion in glomeruli were all ameliorated despite no improvement in hypertension or hyperglycemia. Reasons for the above conflicting results are unclear but possibly attributable, at least in part, to the exclusive reliance on chemical inhibitors or activators of GSK3β, which may possess off-target activities as well as systemic effects. Indeed, due to its ATP competitive property, BIO is also able to block many other kinases involved in diabetes or β cell injury, such as tyrosine kinase 2 (Tyk2) and cyclin dependent kinase 5 (Cdk5) [65,66]. Moreover, sodium nitroprusside is known to have a potent hemodynamic action [67] and this may confound its renal effect in mice. To conclusively define the role of GSK3β in DKD, it is necessary to selectively manipulate the activity of GSK3β in kidney cells, such as podocytes.

In our study, GSK3β hyperactivity worsened, whereas GSK3β silencing or inhibition attenuated podocyte injury elicited by the type 2 diabetic milieu consisting of high ambient insulin and glucose as well as microinflammation resembled by a low-level inflammatory background

of TNF-α and IL-6. In agreement, Paeng et al. [31] also noted that enhanced GSK3β activity caused podocyte apoptosis under high glucose conditions. But it has been elusive how GSK3β mediates diabetic podocyte injury. Type 2 diabetes and its complications like DKD are characterized by both insulin signaling resistance and oxidative stress. GSK3β is situated at the nexus of insulin signaling pathway and Nrf2 pathway. Thus, it is tempting to speculate whether GSK3β regulates both insulin and Nrf2 pathways in diabetic podocyte injury. Based our data and previous findings [22,28], the following GSK3β-driven pathomechanisms seem to contribute.

First, our data indicated that GSK3β is able to phosphorylate IRS-1 at serine 332 as its cognate substrate in podocytes. Phosphorylation of IRS-1 at serine 332 has been known to desensitize the insulin signaling activity [68]. In addition, GSK3β-targeted phosphorylation of IRS-1 at serine 332 could facilitate IRS-1 proteasomal degradation under conditions of insulin resistance, and thus control both the stability and activity of IRS-1 [54]. All these data point to a possible role of GSK3β in regulating the sensitivity of glomerular podocytes, a newly identified type of insulin effector cells [51], to insulin stimulation (Fig. 7).

Second, the present study demonstrated that GSK3β hyperactivity impaired the Nrf2 antioxidant response of podocytes to diabetic injury and mitigated the expression of HO-1 and NQO1 that are capable of quenching the activity of ROS, leading to H_2O_2 accumulation and increased levels of proteins modified by nitration. These effects were abrogated by GSK3β knockdown or inhibitor. In consistency, Dal-Pont et al. [69] found that GSK3β inhibition reduced protein tyrosine nitration in brain specimens in rats with ouabain-induced mania. GSK3β has been shown to directly phosphorylate Nrf2, resulting in both Nrf2 nuclear exclusion and proteasomal degradation [70]. In agreement with our observation, previous studies showed that GSK3β-dictated regulation of Nrf2 plays a key role in governing Nrf2 antioxidant response in other kidney diseases [17,71], and also in podocyte injury in streptozotocin -induced type 1 DKD [22]. DKD is characterized by excess production of ROS and oxidative stress. In line with our finding, overproduction of ROS especially H_2O_2 was found to be induced by hyperglycemia *via* NADPH oxidase 4 in glomerular cells like podocytes [72]. H_2O_2, in turn, suppresses nitric oxide synthase (NOS) activity, decreases the bioavailability of nitric oxide in podocytes and thereby depolymerizes actin cytoskeleton [73]. Moreover, compromised NOS activity may provoke the formation of peroxynitrite [73], which could cause nitration of proteins particularly by tyrosine residues [74], as also shown here in our study. All these oxidative stress may further enhance the activity of the redox-sensitive GSK3β, impair the Nrf2 antioxidant defense and subsequently promote ROS accumulation, thus establishing a vicious cycle (Fig. 7).

In addition, oxidative stress represents a prevailing mechanism in driving premature cellular senescence in many cell types, including glomerular podocytes [75]. ROS, specifically H_2O_2, can cause DNA

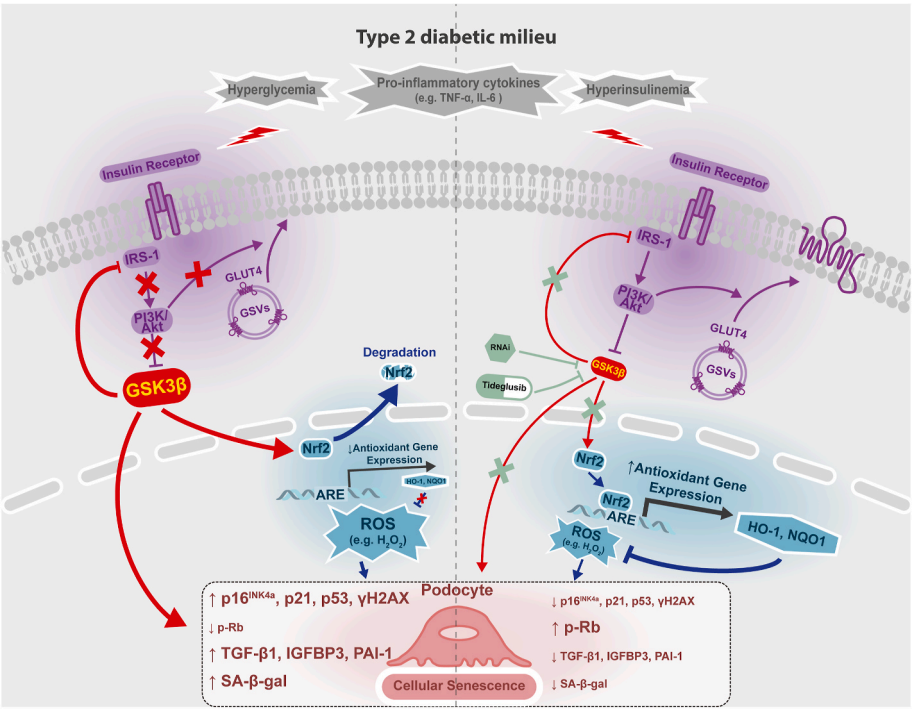

Fig. 7. A schematic diagram illustrates the multifaceted role of the redox-sensitive GSK3β in podocyte injury upon type 2 diabetic insult and the protective effect of targeting GSK3β.

GSK3β is predominantly expressed in glomeruli and highly enriched in glomerular podocytes. The present study demonstrated that GSK3β is hyperactive in podocytes in type 2 diabetic kidney disease, recapitulated *in vitro* by a type 2 diabetic milieu consisting of high ambient insulin and glucose as well as microinflammation resembled by a low-level inflammatory background of TNF-α and IL-6. As a redox-sensitive kinase, GSK3β hyperactivity in podocytes may be primarily caused by diabetes-associated oxidative stress. Subsequently, GSK3β hyperactivity diminishes Nrf2 nuclear accumulation in podocytes, and thereby mitigates the expression of a number of enzymatic antioxidants, including HO-1 and NQO1, resulting in overproduction of reactive oxygen species (ROS), more specifically H_2O_2. This will further promote GSK3β hyperactivity and thus form a vicious cycle. Meanwhile, augmented oxidative stress will cause DNA damage and protein tyrosine nitration and thereby activate the cellular senescence signaling and worsen podocyte senescence, though GSK3β *per se* has been shown to directly drive podocyte senescence signaling. On the other side, as a key transducer of the insulin signaling pathway, GSK3β is able to regulate IRS-1 phosphorylation at Serine 332, which negatively regulates IRS-1 activity. GSK3β hyperactivity causes IRS-1 hyperphosphorylation and thereby de-sensitizes insulin signaling, resulting in reduced inhibitory inhibition of GSK3β and another vicious cycle of GSK3β hyperactivity. De-sensitized insulin signaling also affects the translocation of GLUT4 to the plasma membrane and glucose uptake in podocytes, leading to glucose metabolic reprogramming. All the above pathogenic pathways are involved in diabetic podocyte injury in type 2 diabetes and could be intercepted by genetic targeting of GSK3β *via* RNAi or pharmacological targeting *via* using small molecule inhibitors, such as tideglusib (TDG).
Abbreviations: ARE, antioxidant responsive element; GSVs, GLUT storage vesicles.

damage and DNA double-strand breaks (DSBs) [76]. Consequently, p53-mediated DNA damage response (DDR) is activated [77], leading to upregulation of p21 and $p16^{INK4A}$, which contribute to cell cycle arrest and check point enforcement, ultimately resulting in cellular senescence [78]. In addition, excessive peroxynitrite generation leads to protein tyrosine nitration and contributes to senescence by inactivating crucial enzymes involved in cell metabolism and energy [74]. Indeed, Broadsky et al. [79] demonstrated that ebselen, a peroxynitrite scavenger, was able to mitigate premature cellular senescence in diabetic rats through controlled decrease in protein nitration. As the master regulator of antioxidant responses, Nrf2 possesses a potent anti-senescent activity, as proven by a plethora of work [80–83]. Nrf2 has also been shown to convey the beneficial effect of GSK3 inhibitors, such as lithium, on protecting against senescence or degenerative changes in many organ systems other than the kidney or on promoting longevity in flies [84]. In agreement with our findings that GSK3β regulates the diabetic stress induced premature senescence in glomerular podocytes, recent work reveals that GSK3β plays a key role in podocyte senescence during natural kidney aging [42]. Although GSK3β may directly interact with key senescence signaling mediators like $p16^{INK4A}$ and p53 [85], the present study suggests that the Nrf2 antioxidant response is involved in GSK3β regulation of the diabetes-elicited podocyte senescence.

Our mechanistic model for diabetic podocyte injury merit further validation in future studies using podocyte specific KO of GSK3β in animal models of type 2 DKD. Podocyte-specific KO of GSK3 or only GSK3β in mice has been reported with very different results. Combined KO of GSK3α and β in podocytes resulted in kidney failure under physiological conditions due to severe glomerulopathy, whereas KO of GSK3β alone generated no phenotype. The molecular mechanism responsible for the opposite finding is unknown. But β-catenin, as a typical target of GSK3 signaling, plays a crucial role in maintaining podocyte homeostasis [86], and β-catenin overactivation contributes to podocyte injury [87]. Combined KO of GSK3α and β, as expected, activated β-catenin and disrupted Hippo signaling in podocytes. In contrast, conditional ablation of only GSK3β in podocytes had little effect on β-catenin pathway, as shown by us [16] and by Hurcombe et al. [25]. This is probably attributable to compensation for the loss of GSK3β by GSK3α, which seems to be redundant with GSK3β in mediating Wnt/β-catenin signaling [88]. Collectively, a fine balance of GSK3β inhibition and activation seems essential for kidney health and can be achieved without altering β-catenin activity or causing adverse effects.

Diabetes-associated oxidative stress is not limited to podocytes but also applies to many other glomerular cells, such as glomerular endothelial cells, as also evidenced here by the presence of Nrf2 staining in many glomerular cells other than podocytes (Fig. 6D). Glomerular endothelial dysfunction also contributes to the pathogenesis of DKD, either directly *via* destruction of fenestrated endothelial integrity or indirectly *via* an aberrant cross-talk with podocytes. As a ubiquitously expressed kinase, GSK3β is also expressed by glomerular endothelial cells despite an enriched expression in podocytes. Whether GSK3β is also involved in glomerular endothelial dysfunction and oxidative stress in DKD is a question worthy further investigation.

Furthermore, since GSK3β is a redox-sensitive signaling transducer, the impacts of activating/inactivating Nrf2 dependent response should be taken into account. To this end, the enhanced oxidative stress as a result of Trig inactivation of Nrf2 may cause hyperactivity of the residually expressed GSK3β in GSK3β-silenced podocytes. This may confound the detection of the involvement of Nrf2 in GSK3β regulation of diabetic podocyte injury. Likewise, the improved oxidative stress consequent to tBHQ activation of Nrf2 may lead to hypoactivity of the endogenous GSK3β in S9A-expressing podocytes, which may also be a confounding factor in this study. In-depth studies are warranted to validate these results using GSK3β knockout podocytes in which GSK3β is completely ablated. In addition, GSK3β phosphorylation at multiple sites other than serine 9 may also be involved in diabetic podocyte injury. A thorough phosphorylation identification of GSK3β is necessary for a comprehensive understanding of how GSK3β regulates diabetic podocyte injury.

In summary, GSK3β seems to act as a molecular rheostat in regulating podocyte injury in type 2 DKD. In diabetic podocyte injury, GSK3β is hyperactive and thereby desensitizes the insulin signaling, impairs the Nrf2 antioxidant response and promotes cellular senescence in glomerular podocytes. Our findings suggest that therapeutic targeting of GSK3β may represent a novel strategy in treating podocyte injury and albuminuria in type 2 DKD.

CRediT authorship contribution statement

Mengxuan Chen: Writing – review & editing, Writing – original draft, Methodology, Data curation, Formal analysis, Visualization. **Yudong Fang:** Methodology. **Yan Ge:** Methodology. **Shuhao Qiu:** Methodology. **Lance Dworkin:** Resources. **Rujun Gong:** Writing – review & editing, Writing – original draft, Supervision, Project administration, Methodology, Investigation, Data curation, Formal analysis, Funding acquisition, Resources.

Declaration of competing interest

Part of this work was presented at the ASN Kidney Week in 2023. R. G. has consulted for Reata, Mallinckrodt, and ANI Pharmaceuticals on topics unrelated to this study. All the other authors declared no competing interests.

Data availability

Data will be made available on request.

Acknowledgements

RG was supported in part by the University of Toledo incentive funds and the US National Institutes of Health grant DK133203. The authors are indebted to Dr. M. Chang for assistance with the GSEA analysis.

Appendix A. Supplementary data

Supplementary data to this article can be found online at https://doi.org/10.1016/j.redox.2024.103127.

References

[1] R.Z. Alicic, M.T. Rooney, K.R. Tuttle, Diabetic kidney disease: challenges, progress, and possibilities, Clin. J. Am. Soc. Nephrol. 12 (12) (2017) 2032–2045.
[2] K.R. Tuttle, et al., Diabetic kidney disease: a report from an ADA Consensus Conference, Am. J. Kidney Dis. 64 (4) (2014) 510–533.
[3] 2. Classification and diagnosis of diabetes: standards of medical Care in diabetes-2021, Diabetes Care 44 (Suppl 1) (2021) S15–s33.
[4] D. de Zeeuw, H.J.L. Heerspink, Unmet need in diabetic nephropathy: failed drugs or trials? Lancet Diabetes Endocrinol. 4 (8) (2016) 638–640.
[5] G.L. Bakris, Major advancements in slowing diabetic kidney disease progression: focus on SGLT2 inhibitors, Am. J. Kidney Dis. 74 (5) (2019) 573–575.
[6] R.Z. Alicic, E.J. Johnson, K.R. Tuttle, SGLT2 inhibition for the prevention and treatment of diabetic kidney disease: a review, Am. J. Kidney Dis. 72 (2) (2018) 267–277.
[7] S.C. Palmer, et al., Sodium-glucose cotransporter protein-2 (SGLT-2) inhibitors and glucagon-like peptide-1 (GLP-1) receptor agonists for type 2 diabetes: systematic review and network meta-analysis of randomised controlled trials, BMJ 372 (2021) m4573.
[8] J. Barrera-Chimal, et al., Mineralocorticoid receptor antagonists in diabetic kidney disease - mechanistic and therapeutic effects, Nat. Rev. Nephrol. 18 (1) (2022) 56–70.
[9] 11. Chronic kidney disease and risk management: standards of medical Care in diabetes-2022, Diabetes Care 45 (Suppl 1) (2022) S175–s184.
[10] J.B. McGill, et al., Making an impact on kidney disease in people with type 2 diabetes: the importance of screening for albuminuria, BMJ Open Diabetes Res Care 10 (4) (2022).
[11] M. Oshima, et al., Trajectories of kidney function in diabetes: a clinicopathological update, Nat. Rev. Nephrol. 17 (11) (2021) 740–750.

[12] J.A. Jefferson, S.J. Shankland, R.H. Pichler, Proteinuria in diabetic kidney disease: a mechanistic viewpoint, Kidney Int. 74 (1) (2008) 22–36.
[13] J. Reiser, S. Sever, Podocyte biology and pathogenesis of kidney disease, Annu. Rev. Med. 64 (2013) 357–366.
[14] H. Dai, Q. Liu, B. Liu, Research progress on mechanism of podocyte depletion in diabetic nephropathy, J. Diabetes Res. 2017 (2017) 2615286.
[15] F. Barutta, S. Bellini, G. Gruden, Mechanisms of podocyte injury and implications for diabetic nephropathy, Clin. Sci. (Lond.) 136 (7) (2022) 493–520.
[16] C. Li, et al., The β isoform of GSK3 mediates podocyte autonomous injury in proteinuric glomerulopathy, J. Pathol. 239 (1) (2016) 23–35.
[17] S. Zhou, et al., Genetic and pharmacologic targeting of glycogen synthase kinase 3β reinforces the Nrf2 antioxidant defense against podocytopathy, J. Am. Soc. Nephrol. 27 (8) (2016) 2289–2308.
[18] C. Zhang, et al., HGF alleviates high glucose-induced injury in podocytes by GSK3β inhibition and autophagy restoration, Biochim. Biophys. Acta 1863 (11) (2016) 2690–2699.
[19] S.H. Wang, et al., Cadmium toxicity toward autophagy through ROS-activated GSK-3beta in mesangial cells, Toxicol. Sci. 108 (1) (2009) 124–131.
[20] E. Beurel, S.F. Grieco, R.S. Jope, Glycogen synthase kinase-3 (GSK3): regulation, actions, and diseases, Pharmacol. Ther. 148 (2015) 114–131.
[21] P. Patel, J.R. Woodgett, Glycogen synthase kinase 3: a kinase for all pathways? Curr. Top. Dev. Biol. 123 (2017) 277–302.
[22] Y. Fang, et al., The ketone body β-hydroxybutyrate mitigates the senescence response of glomerular podocytes to diabetic insults, Kidney Int. 100 (5) (2021) 1037–1053.
[23] R.S. Jope, Lithium and GSK-3: one inhibitor, two inhibitory actions, multiple outcomes, Trends Pharmacol. Sci. 24 (9) (2003) 441–443.
[24] C. Li, et al., The redox sensitive glycogen synthase kinase 3β suppresses the self-protective antioxidant response in podocytes upon oxidative glomerular injury, Oncotarget 6 (37) (2015) 39493–39506.
[25] J.A. Hurcombe, et al., Podocyte GSK3 is an evolutionarily conserved critical regulator of kidney function, Nat. Commun. 10 (1) (2019) 403.
[26] L. Lasagni, et al., Podocyte regeneration driven by renal progenitors determines glomerular disease remission and can Be pharmacologically enhanced, Stem Cell Rep. 5 (2) (2015) 248–263.
[27] H. Bao, et al., Fine-tuning of NFκB by glycogen synthase kinase 3β directs the fate of glomerular podocytes upon injury, Kidney Int. 87 (6) (2015) 1176–1190.
[28] X. Liang, et al., Glycogen synthase kinase 3β hyperactivity in urinary exfoliated cells predicts progression of diabetic kidney disease, Kidney Int. 97 (1) (2020) 175–192.
[29] E. Tolosa, et al., A phase 2 trial of the GSK-3 inhibitor tideglusib in progressive supranuclear palsy, Mov. Disord. 29 (4) (2014) 470–478.
[30] S. Lovestone, et al., A phase II trial of tideglusib in Alzheimer's disease, J Alzheimers Dis 45 (1) (2015) 75–88.
[31] J. Paeng, et al., Enhanced glycogen synthase kinase-3β activity mediates podocyte apoptosis under diabetic conditions, Apoptosis 19 (12) (2014) 1678–1690.
[32] G. Armagan, et al., Regulation of the Nrf2 pathway by glycogen synthase kinase-3β in MPP⁺-Induced cell damage, Molecules 24 (7) (2019).
[33] S. Zhang, et al., The roles of GSK-3β in regulation of retinoid signaling and sorafenib treatment response in hepatocellular carcinoma, Theranostics 10 (3) (2020) 1230–1244.
[34] W. Xu, et al., Glycogen synthase kinase 3β dictates podocyte motility and focal adhesion turnover by modulating paxillin activity: implications for the protective effect of low-dose lithium in podocytopathy, Am. J. Pathol. 184 (10) (2014) 2742–2756.
[35] S.J. Shankland, et al., Podocytes in culture: past, present, and future, Kidney Int. 72 (1) (2007) 26–36.
[36] Y. Jin, et al., A systems approach identifies HIPK2 as a key regulator of kidney fibrosis, Nat. Med. 18 (4) (2012) 580–588.
[37] E. Ishida, J.Y. Kim-Muller, D. Accili, Pair feeding, but not insulin, phloridzin, or rosiglitazone treatment, curtails markers of β-cell dedifferentiation in db/db mice, Diabetes 66 (8) (2017) 2092–2101.
[38] B.Y. Peng, et al., A novel and quick PCR-based method to genotype mice with a leptin receptor mutation (db/db mice), Acta Pharmacol. Sin. 39 (1) (2018) 117–123.
[39] W. Ju, et al., Defining cell-type specificity at the transcriptional level in human disease, Genome Res. 23 (11) (2013) 1862–1873.
[40] C. Chen, et al., TBtools: an integrative toolkit developed for interactive analyses of big biological data, Mol. Plant 13 (8) (2020) 1194–1202.
[41] H.J. Baelde, et al., Gene expression profiling in glomeruli from human kidneys with diabetic nephropathy, Am. J. Kidney Dis. 43 (4) (2004) 636–650.
[42] Y. Fang, et al., Age-related GSK3β overexpression drives podocyte senescence and glomerular aging, J. Clin. Invest. 132 (4) (2022).
[43] A.C. Lay, et al., Prolonged exposure of mouse and human podocytes to insulin induces insulin resistance through lysosomal and proteasomal degradation of the insulin receptor, Diabetologia 60 (11) (2017) 2299–2311.
[44] A. Jazwa, et al., Effect of heme and heme oxygenase-1 on vascular endothelial growth factor synthesis and angiogenic potency of human keratinocytes, Free Radic. Biol. Med. 40 (7) (2006) 1250–1263.
[45] F.T. Botros, et al., Increase in heme oxygenase-1 levels ameliorates renovascular hypertension, Kidney Int. 68 (6) (2005) 2745–2755.
[46] H.K. Kim, et al., Cytotoxicity of lipid-soluble ginseng extracts is attenuated by plasma membrane redox enzyme NQO1 through maintaining redox homeostasis and delaying apoptosis in human neuroblastoma cells, Arch Pharm. Res. (Seoul) 39 (10) (2016) 1339–1348.
[47] M.P. Murphy, et al., Guidelines for measuring reactive oxygen species and oxidative damage in cells and in vivo, Nat. Metab. 4 (6) (2022) 651–662.
[48] B.C. Dickinson, C. Huynh, C.J. Chang, A palette of fluorescent probes with varying emission colors for imaging hydrogen peroxide signaling in living cells, J. Am. Chem. Soc. 132 (16) (2010) 5906–5915.
[49] J. Zielonka, et al., Boronate probes as diagnostic tools for real time monitoring of peroxynitrite and hydroperoxides, Chem. Res. Toxicol. 25 (9) (2012) 1793–1799.
[50] Y. Zhang, et al., Diabetes mellitus and Alzheimer's disease: GSK-3β as a potential link, Behav. Brain Res. 339 (2018) 57–65.
[51] R.J. Coward, et al., The human glomerular podocyte is a novel target for insulin action, Diabetes 54 (11) (2005) 3095–3102.
[52] G.I. Welsh, et al., Insulin signaling to the glomerular podocyte is critical for normal kidney function, Cell Metabol. 12 (4) (2010) 329–340.
[53] J. Peng, L. He, IRS posttranslational modifications in regulating insulin signaling, J. Mol. Endocrinol. 60 (1) (2018) R1–r8.
[54] S. Leng, et al., Glycogen synthase kinase 3 beta mediates high glucose-induced ubiquitination and proteasome degradation of insulin receptor substrate 1, J. Endocrinol. 206 (2) (2010) 171–181.
[55] P. Wadhwa, P. Jain, H.R. Jadhav, Glycogen synthase kinase 3 (GSK3): its role and inhibitors, Curr. Top. Med. Chem. 20 (17) (2020) 1522–1534.
[56] J. Shi, et al., Quantifying podocyte number in a small sample size of glomeruli with CUBIC to evaluate podocyte depletion of db/db mice, J. Diabetes Res. 2023 (2023) 1901105.
[57] M. Elshani, et al., Transcription factor NFE2L1 decreases in glomerulonephropathies after podocyte damage, Cells 12 (17) (2023).
[58] B.M. Rush, et al., Genetic or pharmacologic Nrf2 activation increases proteinuria in chronic kidney disease in mice, Kidney Int. 99 (1) (2021) 102–116.
[59] S.E. Nikoulina, et al., Inhibition of glycogen synthase kinase 3 improves insulin action and glucose metabolism in human skeletal muscle, Diabetes 51 (7) (2002) 2190–2198.
[60] M. Lappas, GSK3β is increased in adipose tissue and skeletal muscle from women with gestational diabetes where it regulates the inflammatory response, PLoS One 9 (12) (2014) e115854.
[61] Y. Wang, et al., Inactivation of GSK-3beta by metallothionein prevents diabetes-related changes in cardiac energy metabolism, inflammation, nitrosative damage, and remodeling, Diabetes 58 (6) (2009) 1391–1402.
[62] C.L. Lin, et al., Wnt/beta-catenin signaling modulates survival of high glucose-stressed mesangial cells, J. Am. Soc. Nephrol. 17 (10) (2006) 2812–2820.
[63] M.M. Mariappan, et al., Activation of glycogen synthase kinase 3beta ameliorates diabetes-induced kidney injury, J. Biol. Chem. 289 (51) (2014) 35363–35375.
[64] M.M. Mariappan, et al., Activation of glycogen synthase kinase 3β ameliorates diabetes-induced kidney injury, J. Biol. Chem. 289 (51) (2014) 35363–35375.
[65] L. Marroqui, et al., TYK2, a candidate gene for type 1 diabetes, modulates apoptosis and the innate immune response in human pancreatic beta-cells, Diabetes 64 (11) (2015) 3808–3817.
[66] K.C. Liu, et al., Inhibition of Cdk5 promotes beta-cell differentiation from ductal progenitors, Diabetes 67 (1) (2018) 58–70.
[67] M. Tanahashi, et al., Effects of sodium nitroprusside on renal functions and NO-cGMP production in anesthetized dogs, J. Cardiovasc. Pharmacol. 33 (3) (1999) 401–408.
[68] Z. Liberman, H. Eldar-Finkelman, Serine 332 phosphorylation of insulin receptor substrate-1 by glycogen synthase kinase-3 attenuates insulin signaling, J. Biol. Chem. 280 (6) (2005) 4422–4428.
[69] G.C. Dal-Pont, et al., Inhibition of GSK-3β on behavioral changes and oxidative stress in an animal model of mania, Mol. Neurobiol. 56 (4) (2019) 2379–2393.
[70] P. Rada, et al., SCF/{beta}-TrCP promotes glycogen synthase kinase 3-dependent degradation of the Nrf2 transcription factor in a Keap1-independent manner, Mol. Cell Biol. 31 (6) (2011) 1121–1133.
[71] M. Lu, et al., GSK3β-mediated Keap1-independent regulation of Nrf2 antioxidant response: a molecular rheostat of acute kidney injury to chronic kidney disease transition, Redox Biol. 26 (2019) 101275.
[72] J.C. Jha, et al., Podocyte-specific Nox4 deletion affords renoprotection in a mouse model of diabetic nephropathy, Diabetologia 59 (2) (2016) 379–389.
[73] O. Palygin, et al., Nitric oxide production by glomerular podocytes, Nitric Oxide 72 (2018) 24–31.
[74] M.B. Feeney, C. Schöneich, Tyrosine modifications in aging, Antioxidants Redox Signal. 17 (11) (2012) 1571–1579.
[75] N. Rex, A. Melk, R. Schmitt, Cellular senescence and kidney aging, Clin. Sci. (Lond.) 137 (24) (2023) 1805–1821.
[76] S. Burney, et al., The chemistry of DNA damage from nitric oxide and peroxynitrite, Mutat. Res. 424 (1–2) (1999) 37–49.
[77] G. Achanta, P. Huang, Role of p53 in sensing oxidative DNA damage in response to reactive oxygen species-generating agents, Cancer Res. 64 (17) (2004) 6233–6239.
[78] Q.M. Chen, et al., Molecular analysis of H2O2-induced senescent-like growth arrest in normal human fibroblasts: p53 and Rb control G1 arrest but not cell replication, Biochem. J. 332 (Pt 1) (1998) 43–50 (Pt 1).
[79] S.V. Brodsky, et al., Prevention and reversal of premature endothelial cell senescence and vasculopathy in obesity-induced diabetes by ebselen, Circ. Res. 94 (3) (2004) 377–384.
[80] L. Marquez-Exposito, et al., Oxidative stress and cellular senescence are involved in the aging kidney, Antioxidants 11 (2) (2022).
[81] D. Volonte, et al., Inhibition of nuclear factor-erythroid 2-related factor (Nrf2) by caveolin-1 promotes stress-induced premature senescence, Mol. Biol. Cell 24 (12) (2013) 1852–1862.
[82] X. Luo, et al., An inhibitor role of Nrf2 in the regulation of myocardial senescence and dysfunction after myocardial infarction, Life Sci. 259 (2020) 118199.

[83] H. Yu, et al., Lipid accumulation-induced hepatocyte senescence regulates the activation of hepatic stellate cells through the Nrf2-antioxidant response element pathway, Exp. Cell Res. 405 (2) (2021) 112689.
[84] J.I. Castillo-Quan, et al., Lithium promotes longevity through GSK3/NRF2-dependent hormesis, Cell Rep. 15 (3) (2016) 638–650.
[85] C. López-Otín, et al., Hallmarks of aging: an expanding universe, Cell 186 (2) (2023) 243–278.
[86] H. Kato, et al., Wnt/β-catenin pathway in podocytes integrates cell adhesion, differentiation, and survival, J. Biol. Chem. 286 (29) (2011) 26003–26015.
[87] H. Kato, K. Susztak, Repair problems in podocytes: Wnt, Notch, and glomerulosclerosis, Semin. Nephrol. 32 (4) (2012) 350–356.
[88] B.W. Doble, et al., Functional redundancy of GSK-3alpha and GSK-3beta in Wnt/beta-catenin signaling shown by using an allelic series of embryonic stem cell lines, Dev. Cell 12 (6) (2007) 957–971.